POWER QUALITY IN GRID CONNECTED DISTRIBUTION SYSTEM USING DUAL VOLTAGE SOURCE INVERTER

A Project Report

submitted by

UNNAM CHANDRA KUMAR REDDY

in partial fulfilment of the requirements
for the award of the degree of

MASTER OF TECHNOLOGY

DEPARTMENT OF ELECTRICAL ENGINEERING
INDIAN INSTITUTE OF TECHNOLOGY MADRAS.

JUNE 2017

THESIS CERTIFICATE

This is to certify that the thesis titled **POWER QUALITY IN GRID CONNECTED DISTRIBUTION SYSTEM USING DUAL VOLTAGE SOURCE INVERTER**, submitted by **UNNAM CHANDRA KUMAR REDDY**, to the Indian Institute of Technology, Madras, for the award of the degree of **Master of Technology**, is a bonafide record of the research work done by him under my supervision. The contents of this thesis, in full or in parts, have not been submitted to any other Institute or University for the award of any degree or diploma.

Place: Chennai

Date:

Dr. Mahesh Kumar
Research Guide
Professor
Department of Electrical Engineering
IIT Madras, 600 036

ACKNOWLEDGEMENTS

I would like to sincerely express my profound gratitude to my project guide, Dr Mahesh Kumar for his excellent guidance, motivation and constant support throughout the course of my project. His frequent interactions coupled with his patience have made this endeavour a success. I am also grateful for the laboratory facilities provided by him in the Power Quality Laboratory, Department of Electrical Engineering, which facilitated detailed simulation studies concerned to my work. I greatly value and appreciate the encouragement by my fellow researchers and friends, who were always available as mentors and teachers in testing times. I cherish and retain fond memories of time spent in laboratory, learning research ethics and methodologies from my colleagues. In this context I would like to extend my gratitude towards my fellow mates **Manik Pradhan,** T. Sreekanth, Pruthvi Chaitanya, Y Ram Shankar, Nitin and Leela Krishna.

Besides, I would like to thank my entire M.Tech batch mates Benny, Harsha, Madhav, Hari krishna, Siva Prasad, Saranya, Avinash, Kunal and Subodh who were present to support and celebrate every effort and achievement of mine. I thoroughly enjoyed and cherish the discussions spanning over wide spectrum both related and non related to research, which helped me rejuvenate and keep interest in my work alive.

ABSTRACT

KEYWORDS: Microgrid; voltage source inverter (VSI); parallel operation; power quality (PQ); multifunctional; dual inverters; current control; reactive current; harmonics.

Rapidly growing energy demand and increasing concerns on environment, challenge the conventional power system to accommodate more and more renewable distributed generation (DG) sources. The co-ordinated and controlled operation of these DG units with added storage facilities forms a microgrid system. In a microgrid, power from different renewable energy sources such as fuel cells, photo voltaic (PV) systems, wind energy systems are interfaced to grid and loads using power electronic converters. Moreover, the extensive use of power electronic based equipments, reactive unbalanced and nonlinear loads deteriorates the power quality in power distribution system. In such case, DG units and power electronic converters should also function to compensate for any harmonics in currents drawn by nonlinear loads, so that harmonics will not propagate to other electrical networks connected to point of common coupling (PCC).
The multifunctional grid tied inverters (MFGTIs) are increasingly being used as grid interfacing devices for DG units in microgrid. These inverters simultaneously handle the power flow and address power quality aspects at the interconnected points. The use of ancillary services in these interfacing inverters can significantly enhance their cost effectiveness. However, the use of these inverters for high power applications is limited by the available maximum current rating of semiconductor devices. Therefore, in order to match with high power requirements and to avoid the use of large capacity centralized inverters, parallel operation of inverters is increasingly being suggested.

In this work, dual voltage source inverter is analysed. The control algorithm is derived using instantaneous symmetrical component theory (ISCT) to ensure proportional sharing of active, reactive, unbalance and harmonic power between the inverters. The

proposed control algorithm also compensates the unbalanced nonlinear load and thus makes the grid currents balanced sinusoidal and in phase with respective source voltages. The control strategy is tested with dual inverter connected to a three-phase four-wire distribution system.

TABLE OF CONTENTS

LIST OF TABLES

LIST OF FIGURES

ABBREVIATIONS

PQ	Power Quality
SMPC	Switch Mode Power Converters
RES	Renewable Energy Sources
UPS	Uninterrupted Power Supply
PF	Passive Filter
FACTS	Flexible AC Transmission Systems
CPD	Custom Power Device
DSTATCOM	Distribution Static Synchronous Compensator
DVR	Dynamic Voltage Restorer
UPQC	Unified Power Quality Conditioner
CCM	Current Controlled Mode
VCM	Voltage Controlled Mode
PCC	Point of Common Coupling
VSI	Voltage Source Inverter
DES	Distribution Energy Sources
DVSI	Dual Voltage Source Inverter
SRF	Synchronous Reference Frame
PLL	Phase Locked Loop
UPF	Unity Power Factor
CSI	Current Source Inverter
IGBT	Insulated Gate Bipolar Transistor
PV	Photo Voltaic
MPP	Maximum Power Point
IC	Incremental Conductance
STC	Standard Test Condition
ISCT	Instantaneous Symmetrical Component Theory
MVSI	Main Voltage Source Inverter

AVSI	Auxiliary Voltage Source Inverter
HBCC	Hysteresis Band Current Controller
DG	Distributed Generation

CHAPTER 1

INTRODUCTION

Ideally, the three phase electrical utility is supposed to supply balanced and sinusoidal voltages at the consumer end. Also, the currents drawn by the consumers should be sinusoidal, balanced and in upf with the voltages respectively. If there are any deviations from the above mentioned conditions at the consumer end, then they can be called as the Power Quality (PQ) problems.

The unbalanced inductive loads and increased usage of power electronic switching devices in the applications like switched mode power supply (SMPS), uninterrupted power supply (UPS), rectifers, etc., in the distribution system lead to supply of unbalanced distorted source currents with poor power factor. These kind of PQ problems create negative impact in the system such as excessive neutral current, large neutral voltage w.r.t ground. Also, effects transformers and other electrical equipments by overheating them. Apart from these, voltage related PQ issues arises when their is a switching of excessive capacitive loads such as voltage swell, sag, surges, unbalances, fluctuations etc. These type of PQ problems greatly affect the functioning of sensitive loads, like adjustable speed drives, health care instruments, electronic equipments etc. In recent times, significant number of renewable energy sources (RESs) are being connected to grid with the help of converters (dc-ac or ac-dc-ac) available in power electronics. Besides the inherent intermittent feature of RESs, operating the converters at high switching frequencies exacerbates the PQ problems in the distribution system.

The simple and formal strategies for improving Power Quality (PQ) can be done by passive filters (PFs) which use inductors and capacitors tuned to a specific frequency. But, usage of PFs is much restricted because of many disadvantages that are, quality compensation for only fixed load, performance based on system parameters, need of a new filter for every frequency component, resonance possibility with line reactance.

To overcome the limitations put by PFs, a new kind of devices were developed for improving power quality. These devices are called as FACTS (flexible ac transmission

systems) devices and CPDs (custom power devices) [1]-[5]. Among them, FACTS devices are used in transmission system where as CPDs are used in the distribution system. In these thesis, only CPDs are given importance, as focus is only on the distribution side PQ problems.

1.1 CUSTOM POWER DEVICES (CPDs)

In distribution system, the CPDs are being used for a voltage range of 1-38 kv to alleviate the PQ problems. The devices in the CPD family are Dynamic Voltage Restorer (DVR), Distribution Static Synchronous Compensator (DSTATCOM), Unified Power Quality Conditioner (UPQC), Solid-State Fault Current Limiter (SSFCL) and Solid-State Transfer Switch (SSTS).

1.1.1 Distribution Static Compensator (DSTATCOM)

DSTATCOM is a kind of shunt connected CPD which looks more often on current related PQ issues [1]-[3]. DSTATCOM can be operated in two modes i.e., current controlled mode (CCM), and voltage controlled mode (VCM). In CCM mode it injects

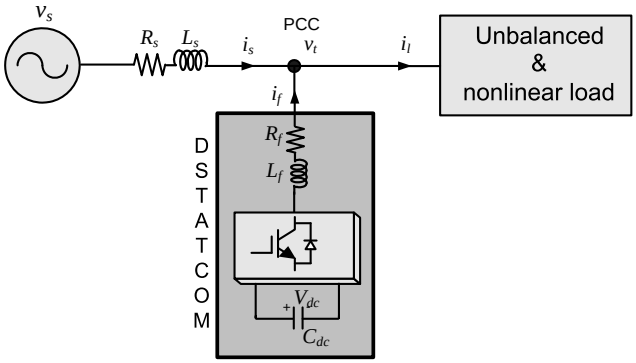

Figure 1.1: Schematic diagram of DSTATCOM

the needed amount of reactive and harmonic current to the load so that it makes the source currents sinusoidal, balanced and harmonic free. In VCM mode, it has the ability to minimize voltage related PQ issues. Schematic diagram of the DSTATCOM in the

distribution system is shown Fig. 1.1. It consists of a voltage source inverter (VSI) supported by a dc link capacitor C_{dc} charged to V_{dc}, which injects the needed current at point of common coupling (PCC) through the interfacing filter ($L_{f)}$) having an internal resistance (R_f).

1.1.2 Dynamic Voltage Restorer (DVR)

DVR is a kind of series connected custom power device which looks after the PQ problems related to voltage such as voltage swell, sag, unbalance and protects the sensitive loads at the load terminal by keeping the voltage in a balanced sinusoidal manner [4]. Schematic diagram of the DVR in the distribution system is shown Fig. 1.2. It consists

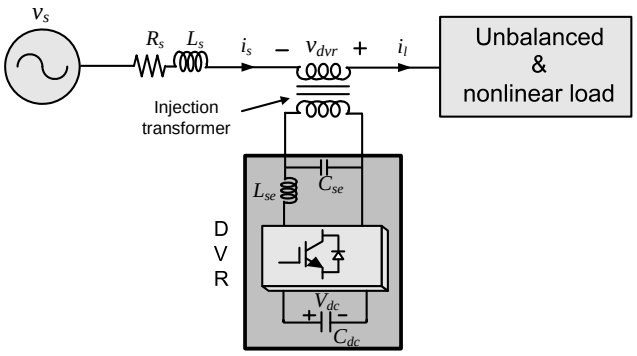

Figure 1.2: Schematic diagram of DVR

of voltage source inverter, transformer which injects voltage in series with the help of dc charged capacitor through VSI and the passive type of filters (L_{se} and C_{se}) which reduces the switching frequency component of VSI. The injected voltage (V_{dvr}) which adds to supply voltage in series makes the load voltage (V_l) free of distortion, keeping sinusoidal with desired magnitude and phase angle.

1.1.3 Unified Power Quality Conditioner (UPQC)

UPQC is kind of device which comprises both series and shunt connected devices connected in back to back through a common dc link [5]. It has the ability to minimize both current and voltage related PQ problems simultaneously, by injecting current through

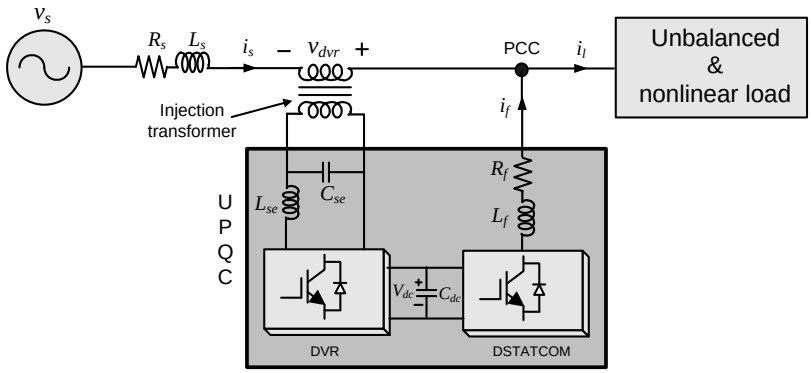

Figure 1.3: Schematic diagram of UPQC

shunt device and voltage through series device. Schematic diagram of the UPQC in the distribution system is shown Fig. 1.3.

1.2 Distribution Energy Sources

With the increasing power demand, the Conventional energy sources confronts problems like fossil fuel depletion, increased carbon foot print, increased losses and poor efficiency. This led to a new kind of power generation at distribution level called as Distribution energy sources (DES) such as wind , solar etc. This type of generation at distribution level helps in reducing the distribution and transmission losses, and also carbon emissions by effectively tapping renewable energy.

This kind of DES are being used in the system for grid inter connection [6], stand alone, peak shavings. This distributed energy sources, apart from supplying power to local load, also supplies power to the grid if the distributed generation is more than the local power consumption.

1.3 Motivation

Of the several PQ problems, voltage kind of problems are not often. In such a case, the DVR and the series part of UPQC may be in standby mode for most of the time.

The other type of current related PQ issues are more often and can be minimized with DSTATCOM by compensating load reactive power.

Because of the several problems being created by conventional energy sources and having the potential renewable energy resources with us, DSTATCOM being supported by renewable energy are on the rise. This renewable energy voltage source inverter compensates reactive power and also supplies active power to the load and makes the system free from PQ problems. But, as there are many advantages with dual voltage source inverter (DVSI), in which one inverter shares load active power and other compensates reactive power, focus in this project is given on DVSI.

1.4 Objectives

Based on the above motivation the following are the objectives of this project work.

1. To model a control algorithm for voltage source inverter such that it compensates the power drawn by unbalanced and non-linear loads and ensures source currents balanced and sinusoidal with the required power factor.

2. To attach a one more shunt connected voltage source inverter to grid which shares load active power with the help of photovoltaic modelled system, which makes the overall system more reliable and flexible.

1.5 Organization of Thesis

In **chapter 1**, different power quality problems and their impact on the load side and on power distribution network is introduced. It briefs about passive type filters for PQ improvement and their limitations. Then, the custom power devices are explained in detail for improving power quality. And then, the motivations and objectives are mentioned.

In **chapter 2**, a detailed literature survey of structure, operating principle and different topologies of DSTATCOM are provided. Also, control strategies for generation of

reference currents for CCM operation of DSTATCOM are presented.

In **chapter 3**, literature survey on PV systems has been done. It includes modelling of PV panel, study of voltage, current and power characteristics of PV panel with changes in irradiance and temperature. Also, different MPP algorithms are included.

In **chapter 4**, dual inverter topology is presented to improve the power quality. In this scheme, the microgrid power injection is performed by one inverter and the other inverter addresses the load compensation. This chapter also discusses the extraction of fundamental positive sequence components of voltages from the distorted PCC voltages using dq0 transformation. The performance of this dual inverter scheme is verified by simulation results.

In **chapter 5**, the important conclusions of the project work are presented. Also, suggestions are given for the future scope of the work.

CHAPTER 2

STRUCTURE, CONTROL AND TOPOLOGIES OF DSTATCOM

In chapter 1, different types of power quality problems and various types of devices that have been used were mentioned. Also, it was given that DSTATCOM can be used for frequently appearing current related PQ issues. In this chapter, the structure, operating principles, different theories for reference generation and different topologies of DSTATCOM in CCM that are available in literature are mentioned.

2.1 STURCTURE AND OPERATING PRINCIPLE

The power circuit diagram of DSTATCOM connected to distribution system with three phase four wire neutral point clamped VSI topology is shown in Fig. 2.1.

In this, source voltages of phases *a,b* and *c* are given as v_{sa}, v_{sb}, v_{sc} respectively. Similarly, the voltages at point of common coupling (PCC) or load voltages are given as v_{ta}, v_{tb}, v_{tc}. At the PCC, source, load and compensator connected altogether. The source currents are i_{sa}, i_{sb}, i_{sc}, load currents are i_{la}, i_{lb}, i_{lc} in the respective phases. The compensator VSI currents are i_{fa}, i_{fb}, i_{fc}. The compensator is connected to PCC through the interfacing resistance and inductance mentioned as R_f and L_f respectively. The DC-link capacitors and voltages across them are shown as $C_{dc1} = C_{dc2} = C_{dc}$ and $V_{dc1} = V_{dc2} = V_{dc}$. The DC link capacitors maintains the dc voltage and also acts as energy storage element which supplies the real power difference between the source and load during the times of transient period.
The main objectives of DSTATCOM are:

1. Compensation of load harmonic currents to make source currents sinusoidal.

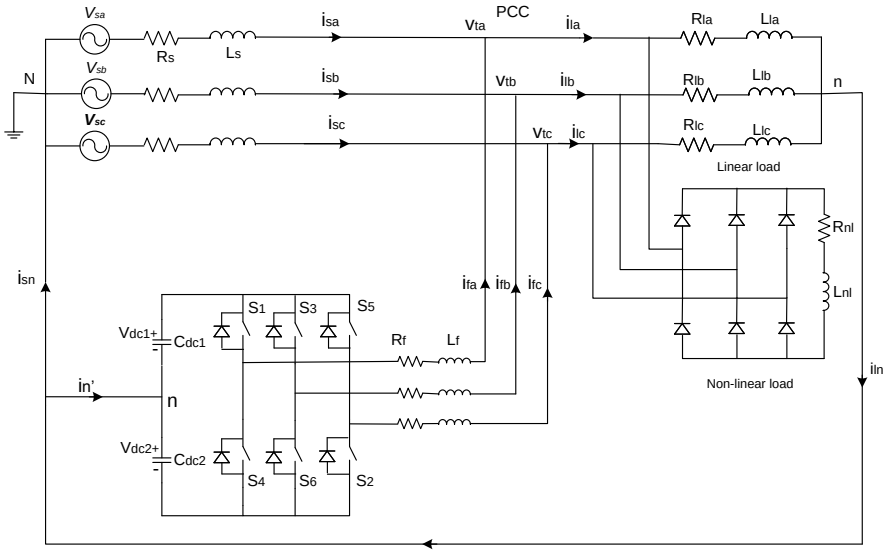

Figure 2.1: Power circuit diagram of three phase DSTATCOM

2. Compensation of reactive component of load currents to make power factor unity at PCC.

3. Compensation of load unbalances to make source neutral current zero. Therefore, a DSTATCOM injects currents at PCC to make the source currents balanced, sinusoidal, and in phase with the respective phase voltages at PCC.

2.2 GENERATION OF REFERENCE CURRENTS

In any active power filter, selection of the control theory plays a significant role in its compensation performance. There are many theories mentioned in the literature for the generation of reference quantities. The most familiar in them are instantaneous reactive power theory [7], synchronous reference theory [10] and instantaneous symmetrical component theory [8],[9]. These theories are explained in the following section.

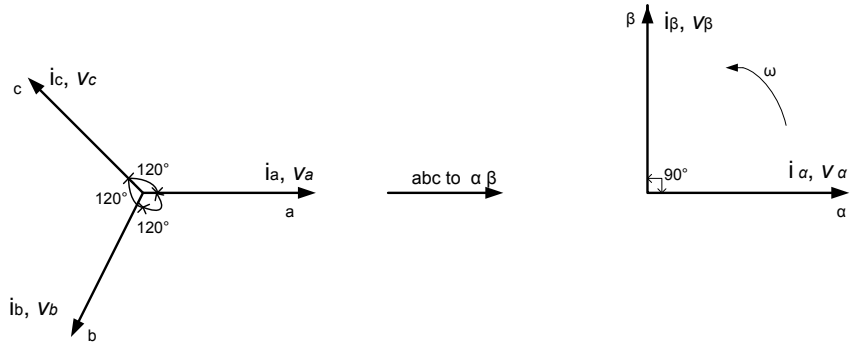

Figure 2.2: abc to $\alpha\beta$ transformation

2.2.1 Instantaneous Reactive Power Theory

Using this theory, a mathematical equation for instantaneous reactive power can be formulated which compensates the reactive power both in steady state and transient conditions [7]. These mathematical equations are formulated using instantaneous voltage and current values. Using the Clark's transformation the phase voltage of *abc* are translated to α-β stationary axis as shown in Fig. 2.2.

The transformed equations in α-β axis are

$$\begin{bmatrix} v_\alpha(t) \\ v_\beta(t) \end{bmatrix} = \sqrt{\frac{2}{3}} \begin{bmatrix} 1 & \frac{-1}{2} & \frac{-1}{2} \\ 0 & \frac{\sqrt{3}}{2} & \frac{-\sqrt{3}}{2} \end{bmatrix} \begin{bmatrix} v_a(t) \\ v_b(t) \\ v_c(t) \end{bmatrix} \tag{2.1}$$

$$\begin{bmatrix} i_\alpha(t) \\ i_\beta(t) \end{bmatrix} = \sqrt{\frac{2}{3}} \begin{bmatrix} 1 & \frac{-1}{2} & \frac{-1}{2} \\ 0 & \frac{\sqrt{3}}{2} & \frac{-\sqrt{3}}{2} \end{bmatrix} \begin{bmatrix} i_a(t) \\ i_b(t) \\ i_c(t) \end{bmatrix} \tag{2.2}$$

The instantaneous real power and instantaneous reactive power in α-β frame using the instantaneous voltage and current in α-β are given as

$$p = v_\alpha i_\alpha + v_\beta i_\beta \tag{2.3}$$

$$q = v_\alpha i_\beta - v_\beta i_\alpha. \tag{2.4}$$

Thus, instantaneous reacive power in *abc* form from the equations (2.1), (2.2) and (2.4) can be given as

$$q = -\frac{1}{\sqrt{3}}\left[(v_a - v_b)\, i_c + (v_b - v_c)\, i_a + (v_c - v_a)\, i_b\right], \tag{2.5}$$

Now, from the equations (2.3) and (2.4) instantaneous real and reactive powers in α-β frame can be written as

$$\begin{bmatrix} p \\ q \end{bmatrix} = \begin{bmatrix} v_\alpha & v_\beta \\ -v_\beta & v_\alpha \end{bmatrix} \begin{bmatrix} i_\alpha \\ i_\beta \end{bmatrix}, \tag{2.6}$$

The above equation (2.6) can also be written as

$$\begin{aligned} \begin{bmatrix} i_\alpha \\ i_\beta \end{bmatrix} &= \begin{bmatrix} v_\alpha & v_\beta \\ -v_\beta & v_\alpha \end{bmatrix}^{-1} \begin{bmatrix} p \\ q \end{bmatrix} \\ &= \frac{1}{v^2 + v_\beta^2} \begin{bmatrix} v_\alpha & -v_\beta \\ v_\beta & v_\alpha \end{bmatrix} \begin{bmatrix} p \\ q \end{bmatrix} \\ &= \begin{bmatrix} i_{\alpha\, p} \\ i_{\beta\, p} \end{bmatrix} + \begin{bmatrix} i_{\alpha\, q} \\ i_{\beta\, q} \end{bmatrix} \end{aligned} \tag{2.7}$$

The different terms in the above equation (2.7) are given as

instantaneous α axis active current $i_{\alpha\, p} = \frac{v_\alpha p}{v_\alpha^2 + v_\beta^2}$

instantaneous α axis reactive current $i_{\alpha\, q} = -\frac{v_\beta q}{v_\alpha^2 + v_\beta^2}$

instantaneous β axis active current $i_{\beta\, p} = \frac{v_\beta p}{v_\alpha^2 + v_\beta^2}$

instantaneous β axis reactive current $i_{\beta\, q} = \frac{v_\alpha q}{v_\alpha^2 + v_\beta^2}$

Thus, in α-β frame the instantaneous powers can be given as

$$\begin{aligned}\begin{bmatrix} p_\alpha \\ p_\beta \end{bmatrix} &= \begin{bmatrix} v_\alpha i_\alpha \\ v_\beta i_\beta \end{bmatrix} \\ &= \begin{bmatrix} v_\alpha i_{\alpha\,p} \\ v_\beta i_{\beta\,p} \end{bmatrix} + \begin{bmatrix} v_\alpha i_{\alpha\,q} \\ v_\beta i_{\beta\,q} \end{bmatrix}\end{aligned} \tag{2.8}$$

$$p = \frac{v_\alpha^2}{v_\alpha^2+v_\beta^2}p + \frac{v_\beta^2}{v_\alpha^2+v_\beta^2}p + \frac{-v_\alpha v_\beta}{v_\alpha^2+v_\beta^2}q + \frac{v_\alpha v_\beta}{v_\alpha^2+v_\beta^2}q$$

$$p = p_{\alpha\,p} + p_{\beta\,p} + p_{\alpha\,q} + p_{\beta\,q} = p_\alpha + p_\beta$$

where

instantaneous α axis active power $p_{\alpha\,p} = \frac{v_\alpha^2 p}{v_\alpha^2+v_\beta^2}$

instantaneous α axis reactive power $p_{\alpha\,q} = -\frac{v_\alpha v_\beta q}{v_\alpha^2+v_\beta^2}$

instantaneous β axis active power $p_{\beta\,p} = \frac{v_\beta^2 p}{v_\alpha^2+v_\beta^2}$

instantaneous β axis reactive current $p_{\beta\,q} = \frac{v_\alpha v_\beta q}{v_\alpha^2+v_\beta^2}$

Using (2.6), the filter current components in terms of power and voltage can be written as

$$\begin{bmatrix} i_{f\alpha}^* \\ i_{f\beta}^* \end{bmatrix} = \begin{bmatrix} v_\alpha & v_\beta \\ -v_\beta & v_\alpha \end{bmatrix}^{-1} \begin{bmatrix} p_f \\ q_f \end{bmatrix} \tag{2.9}$$

where $i_{f\alpha}^*$ and $i_{f\beta}^*$ are the reference filter currents , p_f and q_f are the powers to be compensated.

As p and q are the instantaneous real and reactive load powers, they can also be defined as $p = \overline{p} + \widetilde{p}$ and $q = \overline{q} + \widetilde{q}$. The terms $\overline{p}$ and $\widetilde{p}$ are the dc and ac components of p, whereas $q = \overline{q}$ and $\widetilde{q}$ are dc and ac components of q.

By selecting $p_f = \widetilde{p}$ and $q_f = \overline{q} + \widetilde{q}$, the instantaneous harmonic active current, instantaneous reactive current having both fundamental and harmonic components can be compensated.

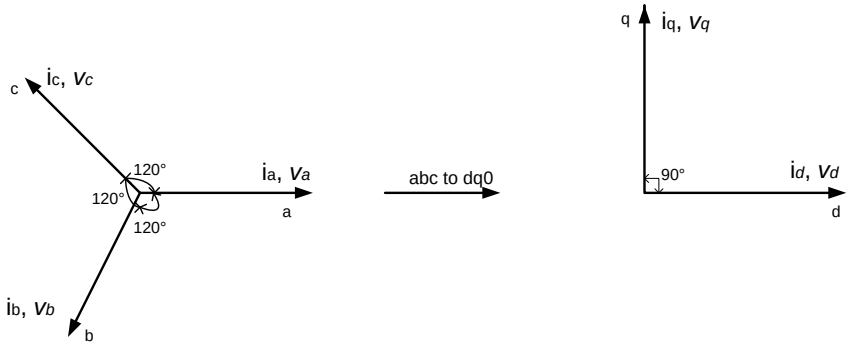

Figure 2.3: abc to $dq0$ transformation

2.2.2 Synchronous Reference Frame Theory

The synchronous reference frame (SRF) theory or dq theory is based on the time domain reference signal estimation techniques. The basic structure of SRF controller consists of direct dq and inverse dq Park transformations. The refernce frame transformations are obtained from a three phase abc stationary system to the direct axis and quadrature axis rotating coordinate system (dq system). The three phase stationary space vectors are transformed into the two axis $dq0$ reference frame, as given in Fig. 2.3.

$$\begin{bmatrix} v_d \\ v_q \\ v_0 \end{bmatrix} or \begin{bmatrix} i_d \\ i_q \\ i_0 \end{bmatrix} = \sqrt{\frac{2}{3}} \begin{bmatrix} \cos(\omega t) & \cos(\omega t - 120°) & \cos(\omega t + 120°) \\ -\sin(\omega t) & -\sin(\omega t - 120°) & \sin(\omega t + 120°) \\ \frac{1}{\sqrt{2}} & \frac{1}{\sqrt{2}} & \frac{1}{\sqrt{2}} \end{bmatrix} \begin{bmatrix} v_a \\ v_b \\ v_c \end{bmatrix} or \begin{bmatrix} i_a \\ i_b \\ i_c \end{bmatrix} \tag{2.10}$$

The ouput signals from dq transformation depend on the phase locked loop (PLL) performannce. The PLL loop provides the rotation speed (rad/sec) of the rotating reference frame, where ωt is set as fundamental frequency component. Depending on the fundamental, harmonics and negative sequence components in voltages and currents, the dq components have different frequencies. The dq components having both dc and ac components are expressed as following:

$$i_{Ld} = \bar{i}_{Ld} + \widetilde{i}_{Ld} = \bar{i}_{Lq} + \widetilde{i}_{Lq}$$

The dc components $\bar{i}_{Ld}$ and $\bar{i}_{Lq}$ correspond to the fundamental positive sequence load currents and the ac components $\widetilde{i}_{Ld}$ and $\widetilde{i}_{Lq}$ correspond to the load current har-

monics. The component $\bar{i}_{Lq}$ corresponds to the reactive power drawn by the load. The references for the compensator can be obtained as follows:

$$i^*_{fd} = -\widetilde{i}_{Ld}, i^*_{fq} = -\bar{i}_{Lq} - \widetilde{i}_{Lq}, i^*_{f0} = -i_{L0}.$$

The references for shunt active filter in abc reference frame can be obtained as follows:

$$\begin{bmatrix} i^*_{fa} \\ i^*_{fb} \\ i^*_{fc} \end{bmatrix} = \sqrt{\frac{2}{3}} \begin{bmatrix} \cos(\omega t) & -\sin(\omega t) & \frac{1}{\sqrt{2}} \\ \cos(\omega t - 120^\circ) & -\sin(\omega t - 120^\circ) & \frac{1}{\sqrt{2}} \\ \cos(\omega t + 120^\circ) & -\sin(\omega t + 120^\circ) & \frac{1}{\sqrt{2}} \end{bmatrix} \begin{bmatrix} i^*_{fd} \\ i^*_{fq} \\ i^*_{f0} \end{bmatrix} \quad (2.11)$$

The calculation of reference currents using this approach is not affected by voltage unbalance and/or distortion. However, PLL is used in this method to get the transformation angle (ωt) from the supply voltage, so this will affect the performance when the supply voltages are unbalanced and/or distorted. This method involves complex transformations and its implementation in real time is difficult.

2.2.3 Instantaneous Symmetrical Component Theory

The theory of instantaneous symmetrical component theory can be used for load balancing, harmonic suppression and power factor correction. also, control algorithm based on this theory can partially or fully compensate any kind of unbalance and harmonic in the load with high bandwidth current sources to track the filter reference currents. According to symmetrical component theory, any three phase instantaneous quantities can be expressed into positive, negative and zero sequences using the following:

$$\begin{bmatrix} i^0_{sa} \\ i^+_{sa} \\ i^-_{sa} \end{bmatrix} or \begin{bmatrix} v^0_{sa} \\ v^+_{sa} \\ v^-_{sa} \end{bmatrix} = \frac{1}{3} \begin{bmatrix} 1 & 1 & 1 \\ 1 & \alpha & \alpha^2 \\ 1 & \alpha^2 & \alpha \end{bmatrix} \begin{bmatrix} i_{sa} \\ i_{sa} \\ i_{sa} \end{bmatrix} or \begin{bmatrix} v_{sa} \\ v_{sa} \\ v_{sa} \end{bmatrix} \quad (2.12)$$

In the equation (2.12), +, $-$ and 0 indicates positive, negative and zero sequence components respectively. The quantity α is complex operator and it is equal to e^{j120}. The instantaneous positive sequence (i^+_{sa}) and instantaneous negative sequence (i^-_{sa}) are complex conjugates of each other and zero sequence (i^0_{sa}) is a real quantity which is zero if the currents are balanced.

Assuming that source voltages to be balanced in the three phase four wire system like in pq theory and for supply currents to be balanced, neutral current to be zero. Therefore

$$i_{sa} + i_{sb} + i_{sc} = 0. \tag{2.13}$$

The angle between the positive sequence component of the source current (i_{sa}^{+}) and the source voltage (v_{sa}^{+}) is same as the power factor angle (ϕ^{+}) between the balanced source currents and voltages. This power factor angle can be explicitly set to any desired value in the control algorithm. However, it is not directly expressed in the pq theory described earlier. By assuming that phase of the (i_{sa}^{+}) lags that of (v_{sa}^{+}) by an angle (ϕ^{+}), we can write

$$\angle(v_{sa} + \alpha v_{sb} + \alpha^2 v_{sc}) = \angle(i_{sa} + \alpha i_{sb} + \alpha^2 i_{sc}) + \phi^{+}. \tag{2.14}$$

After substituting the α and α^2 values in the equation (2.14), it can be written as:

$$\angle\big[(v_{sa} - \frac{1}{2}v_{sb} - \frac{1}{2}v_{sc}) - j\frac{\sqrt{3}}{2}(v_{sb} - v_{sc})\big] = \angle\big[(i_{sa} - \frac{1}{2}i_{sb} - \frac{1}{2}i_{sc}) - j\frac{\sqrt{3}}{2}(i_{sb} - i_{sc})\big] + \phi^{+} \tag{2.15}$$

By equating angles of equation (2.15) one can write as:

$$\tan^{-1}\left(\frac{K_1}{K_2}\right) = \tan^{-1}\left(\frac{K_3}{K_4}\right) + \phi^{+} \tag{2.16}$$

where

$$K_1 = \tfrac{\sqrt{3}}{2}(v_{sb} - v_{sc})\ ,\ K_2 = (v_{sa} - \tfrac{1}{2}v_{sb} - \tfrac{1}{2}v_{sc})$$

$$K_3 = \tfrac{\sqrt{3}}{2}(i_{sb} - i_{sc})\ ,\ K_4 = (i_{sa} - \tfrac{1}{2}i_{sb} - \tfrac{1}{2}i_{sc})$$

Taking tangents on both sides of equation (2.16), we get

$$\frac{K_1}{K_2} = \tan\big[\tan^{-1}(\frac{K_3}{K_4}) + \phi^{+}\big] = \frac{K_3/K_4 + \tan\phi^{+}}{1 - (K_3/K_4)\tan\phi^{+}} \tag{2.17}$$

Substituting values of K_1, K_2, K_3 and K_4 in (2.17), we get

$$(v_{sb} - v_{sc} - 3\gamma(v_{sa} - v_0)i_{sa} + (v_{sc} - v_{sa} - 3\gamma(v_{sb} - v_0)i_{sb} + (v_{sa} - v_{sb} - 3\gamma(v_{sc} - v_0)i_{sc} = 0 \tag{2.18}$$

where $\gamma = \tan\phi^+/\sqrt{3}$. For UPF operation, $\phi^+ = 0$ i.e., $\gamma = 0$. In the balanced circuit the instantaneous power is constant, while in the unbalanced circuit it has a double frequency component in addition to the dc or mean value. Also, the presence of harmonics adds higher frequency oscillating components of the instantaneous power. The objective of the compensator is to supply the oscillating component of the instantaneous load power, while the source supplies the average value of the load power (P_{lavg}). Therefore, average load power is given as following:

$$v_{sa}i_{sa} + v_{sb}i_{sb} + v_{sc}i_{sc} = P_{lavg} \tag{2.19}$$

As the harmonic component present in the load does not require any real power, the source supplies only real power require for load. The average load power can be calculated using moving average filter. Now by combining equations (2.13), (2.18) and (2.19), the reference source currents can be written as follows

$$\begin{bmatrix} i^*_{sa} \\ i^*_{sb} \\ i^*_{sc} \end{bmatrix} = M^{-1} \begin{bmatrix} 0 \\ 0 \\ P_{lavg} \end{bmatrix} \tag{2.20}$$

where

$$M = \begin{bmatrix} 1 & 1 & 1 \\ (v_{sb} - v_{sc} - 3\gamma(v_{sa} - v_0) & (v_{sc} - v_{sa} - 3\gamma(v_{sb} - v_0) & (v_{sa} - v_{sb} - 3\gamma(v_{sc} - v_0) \\ v_{sa} & v_{sb} & v_{sc} \end{bmatrix}$$

The reference compensator currents are given as

$$\begin{aligned} i^*_{fa} &= i_{la} - i^*_{sa} = i_{la} - \frac{(v_{sa} - v_0) + \gamma(v_{sb} - v_{sc})}{\Delta_1}(P_{lavg}) \\ i^*_{fb} &= i_{lb} - i^*_{sb} = i_{lb} - \frac{(v_{sb} - v_0) + \gamma(v_{sc} - v_{sa})}{\Delta_1}(P_{lavg}) \\ i^*_{fc} &= i_{lc} - i^*_{sc} = i_{lc} - \frac{(v_{sc} - v_0) + \gamma(v_{sa} - v_{sb})}{\Delta_1}(P_{lavg}) \end{aligned} \tag{2.21}$$

where

$$\Delta_1 = \left[\sum_{j=a,b,c} v^2_{sj}\right] - 3v_0^2, v_0 = \frac{1}{3}\sum_{j=a,b,c} v_{sk}, \gamma = \tan\phi^+/\sqrt{3}$$

The average power supplied by the source according to the above equation will be equal to the average power required by the load. In addition to the average load power, the source has to supply VSI losses also. When the inverter loss P_{loss} is also included in (2.21), the modified compensator currents become

$$i_{fa}^{*} = i_{la} - i_{sa}^{*} = i_{la} - \frac{(v_{sa} - v_0) + \gamma(v_{sb} - v_{sc})}{\Delta_1}(P_{lavg} + P_{loss})$$

$$i_{fb}^{*} = i_{lb} - i_{sb}^{*} = i_{lb} - \frac{(v_{sb} - v_0) + \gamma(v_{sc} - v_{sa})}{\Delta_1}(P_{lavg} + P_{loss}) \tag{2.22}$$

$$i_{fc}^{*} = i_{lc} - i_{sc}^{*} = i_{lc} - \frac{(v_{sc} - v_0) + \gamma(v_{sa} - v_{sb})}{\Delta_1}(P_{lavg} + P_{loss})$$

The term P_{lavg} can be obtained using simple moving average filter over a half cycle as the oscillating part of the real power has frequency which is the double the system frequency and the P_{loss} is obtained from the PI controller. The error between the reference dc voltage and actual dc voltage is processed through PI controller to get P_{loss}. This will control the dc link voltage by adjusting the small amount of real power absorbed by the shunt inverter. This small amount of real power is adjusted by changing the amplitude of the fundamental component of the reference current. The ac source provides some ac current to recharge the capacitor. Thus, in addition to reactive and harmonic component, the reference current of the shunt active filter has to contain some amount of active current as compensating current. The active compensating current flowing through the shunt active filter regulates the dc capacitor voltage [9].

When the source voltages used for generating the shunt filter current references are unbalanced and distorted, the shunt algorithm results in erroneous compensation. To remove the limitation, fundamental positive sequence voltages $v_{sa1}^{+}(t)$, $v_{sb1}^{+}(t)$ and $v_{sc1}^{+}(t)$ of the PCC voltages are extracted and are used in the shunt algorithm [11]. Then the expression for the reference compensator currents is as follows

$$i^*_{fa} = i_{la} - i^*_{sa} = i_{la} - \frac{v^+_{sa1} + \gamma^+(v^+_{sb1} - v^+_{sc1})}{\Delta^+_1}(P_{lavg} + P_{loss})$$

$$i^*_{fb} = i_{lb} - i^*_{sb} = i_{lb} - \frac{v^+_{sb1} + \gamma^+(v^+_{sc1} - v^+_{sa1})}{\Delta^+_1}(P_{lavg} + P_{loss}) \tag{2.23}$$

$$i^*_{fc} = i_{lc} - i^*_{sc} = i_{lc} - \frac{v^+_{sc1} + \gamma^+(v^+_{sa1} - v^+_{sb1})}{\Delta^+_1}(P_{lavg} + P_{loss})$$

where

$$\Delta^+_1 = \sum_{j=a,b,c} (v^+_{sj1})^2, \gamma^+ = \tan\phi^+/\sqrt{3}$$

Out of the several theories, instantaneous symmetrical component theory with the extraction fundamental fundamental positive sequence components is simple in formulation and devoid of ambiguity over the the definition of various power terms. The compactness of its control and its flexibility to work under all source voltage and load current circumstances make the scheme very attractive to implement in real time.

2.3 VSI TOPOLOGIES FOR DSTATCOM APPLICATIONS

Voltage source inverters are used in the DSTATCOM applications to track the reference quantities being generated. Instead of VSI, current source inverters (CSIs) are also used. However, VSI is preferred over the CSI. This is because that CSIs use bulky and heavy dc inductor, have high dc link losses, need voltage clamp circuit and have reduced efficiency at the nominal operating point as compared to VSI. Also, mean time to failure (MTTF) is very less in CSI, which is an important consideration in industrial applications. The insulated gate bipolar transistor (IGBT) used in VSI, inherently comes with a free-wheeling diode, thus making it cost effective compared to the IGBTs used in CSI. In this section, different two level VSI topologies for DSTATCOM applications [12] are discussed along with merits and demerits.

2.3.1 Neutral Point Clamped VSI Topology

The power circuit of the neutral clamped VSI topology is shown in the Fig. 2.4. This

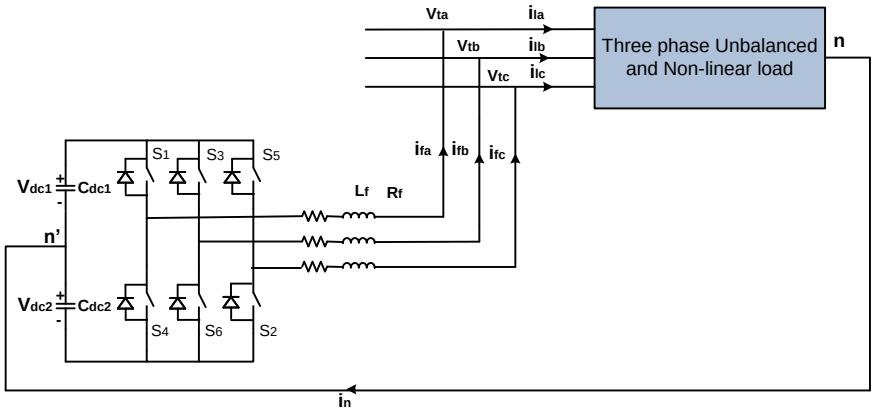

Figure 2.4: Power circuit of neutral point clamped VSI topology

type of topology consists of two dc storage capacitors and the junction (n') of the two capacitors is connected to the neutral of the load. This neutral allows the path for zero sequence current and therefore the three injected currents can be independently controlled. Each leg of the VSI connected to the PCC through a interfacing inductor. The topology consists of six IGBT switches in total as shown in Fig. 2.4. The major drawback in this topology is the requirement for balancing the dc link voltages across the two capacitors. The voltage imbalance is of minor nature whenever the zero sequence current in the neutral wire contains only ac components. However, the problem becomes compounded when neutral contains dc components. The topology fails if the load current contains dc components. The dc component current injection through the capacitors has the effect of charging one of the capacitors above its reference value and discharging the other one below the reference value. Hence, results in dangerously high voltages across the some of the switches. Also, the performance of the compensator degrades due its loss of tracking ability. An alternating topology has been proposed in, where two quadrant chopper is used to equalise voltage across the capacitors. But this topology increases the number of switches and the control becomes complex.

2.3.2 Four Leg VSI Topology

The power circuit of the four leg VSI topology is shown in Fig. 2.5. In this topology, only one dc storage unit is required. Three legs of the VSI are used to track the three phase currents and the fourth leg is connected to load neutral through a reactance to track the negative of zero sequence current. The reference current for the fourth leg is the negative sum of the three phase load currents. This topology can handle the dc component in the load current as it is nullified by tracking the neutral current in the fourth leg of VSI. As fourth leg of VSI is used to track the negative of the zero sequence current, the VSI need to be higher bandwidth one to track the neutral current. The advantage of this topology over the neutral clamped topology is that requires only one capacitor for the storage purpose. The drawbacks are,it requires a high number of VSI legs and switches and cannot be controlled independently.

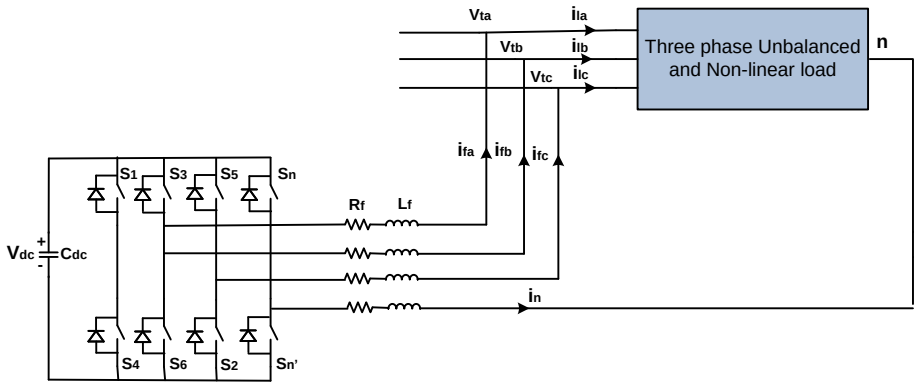

Figure 2.5: Power circuit of four leg VSI topology

2.3.3 H-Bridge VSI Topology

The schematic diagram of H-brige VSI topology is shown in Fig. 2.6. It contains the H-bridge VSI that are connected to a common dc storage capacitor. Each switch in the figure represents a power semiconductor device and an anti-parallel diode combination. Three H-bridge inverters and three interfacing transformers are used to realize the circuit. This topology helps in injecting the filter currents independent of each other. The

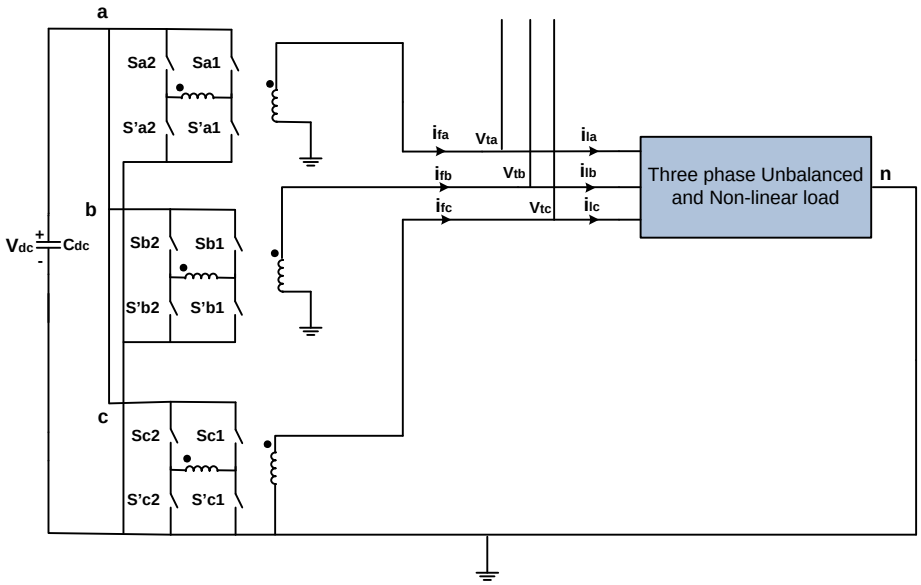

Figure 2.6: Schematic circuit of H-Bridge VSI topology

transformers provide isolation and also prevent dc capacitor being shorted due to operation various switches. This topology has the drawback that it will fail if load draws any dc current. The dc current will saturate the transformers causing heating and increased losses thereby reducing the life of transformers. Also, this topology requires highest number of power semiconductor switches (twelve) compared to other topologies, thus increasing the switching losses ion VSI.

2.4 Summary

In this chapter, principle and operation of DSTATCOM has been presented in detail. The various control schemes to generate reference currents have also discussed. Out of the various theories available for operation DSTATCOM in literature, the instantaneous symmetrical component theory with the extraction of fundamental positive sequence components is simple to formulate and its flexibility to work under all load current and source voltage circumstances make it very attractive choice to implement in a real time system. Also various topologies for the DSTATCOM applications are presented in detail.

CHAPTER 3

MODELLING OF PHOTOVOLTAIC SYSTEM

Owing to the increased awareness of greenhouse gases emission, continuous depletion of fossil fuels and the need for sustainability, renewable sources such as solar, wind, etc., have been studied in recent years. Among them solar power generation is considered as on of the most potential energy source. Photovoltaic (PV) panels are being used to generate solar electric power. These PV panels have non-linear I-V characteristics. The power generation varies throughout the day depending on the irradiance and temperature. The PV power can be varied from zero to maximum at a given weather condition depending on the operating voltage and current of the PV panel. Therefore, it is much required to operate the PV panel at maximum power point (MPP) at all the varying weather conditions. Several control algorithms are available in the literature to operate PV panel at MPP [13].

3.1 Photovoltaic System

Photovoltaics is method of generating electric power by converting solar energy into direct current (DC) electricity using the semiconductors that exhibit the photovoltaic effect. The primary element in solar power generation is the solar cell or PV cell that converts solar radiation into direct electricity. As the power generation from PV cell is less, these cells are interconnected to generate more power and called as PV module. Multiple PV modules are joined together either in parallel or in series or both to form an array. Generally, larger the area of the module or array, more is the electricity generated. The structures of PV cell, module and array are shown in Fig. 3.1.

Photovoltaic Cell: PV cell is the basic p-n junction semiconductor device that converts solar energy into electricity when exposed to light. When radiation falls on the

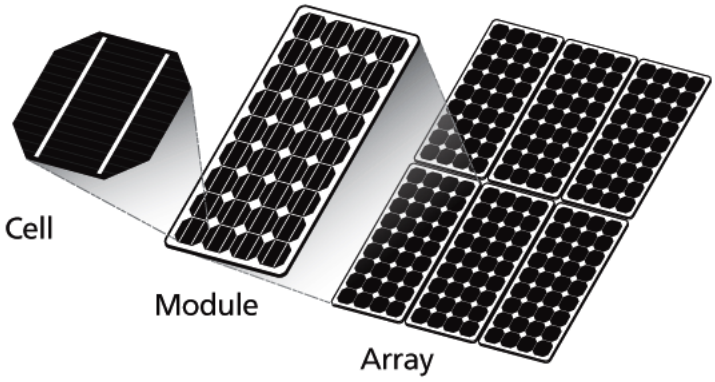

Figure 3.1: PV cell, module and array

surface of the cell, an electric field gets generated inside the cell. In this process positive and negative charge carriers separated from the p-n junction semiconductor, these charge carriers generate current in the presence of electric field when the cell get connected to external circuit. The generated current depends on the solar radiation. If the intensity of solar radiation is more, more number of charge carriers can be unleashed from the PV cell and results in more amount of power generation. This process is called as photovoltaic effect. A PV cell can either be in circular or rectangular or square in construction.

Photovoltaic Module: The heart of the every PV system is the array of photovoltaic modules. The output of a single PV cell is very less around 0.5 V. Therefore, PV modules (also called PV panels) are formed by connecting several PV cells in series to get high voltage and in parallel to get high currents. In case of partial or total shading, diodes are used separately to avoid reverse currents. Reverse currents makes power waste and also lead to overheating of shaded cells and create hotspots. At high temperatures PV cells generates less power, therefore proper ventilation is being provided by service providers behind the PV modules.

Photovoltaic Array: A photovoltaic array (also called solar array) consists of multiple PV modules to convert solar radiation into usable electricity. The power generated by the single PV module is not enough to meet the power requirements of residential, com-

mercial or industrial applications. Thus the modules in the PV array are first connected in series to get the required voltage and then the individual modules are connected in parallel to make system to generate more current. The total DC watts being generated by the PV array depends on the number of modules present in the system. However, the inverter connected to PV array finally governs the amount of AC watts that can be distributed to loads [13].

3.2 Basic Parameters of PV Cell

Photovoltaic cells exhibits a non-linear P-V and I-V characteristics which vary with solar temperature (T) and solar irradiance (S). Several equivalent circuit models of PV cell have been discussed in literature. A general single diode PV model, which consists of a photo current source, a parallel resistor representing a leakage current, a diode, and a series resistor describing the internal resistance to the current flow is considered in this study. The modelling of PV cell and its electrical characteristics are discussed in detail later in this chapter. The electrical characteristics of the PV panel are described as a relation between the panel voltage and current, and panel voltage and power as shown in the Fig. 3.2. it shows the PV panel has non-linear characteristics and the output power of PV panel can be varied from zero to maximum value. Therefore, to effectively use the PV panels, it is always advisable to operate the PV panel at MPP. The operation and performance of the PV cell can be described through several electrical quantities. These quantities include, the cell current under short circuit conditions, the cell voltage under open circuit conditions, and the cell voltage, current and power at MPP. The PV cell can be characterized by the following fundamental parameters [13].

Short Circuit Current (I_{sc}): Short circuit current is the maximum possible current a PV cell can generate at the given weather conditions when cell voltage is zero as shown in Fig. 3.2. This case occurs by shorting the positive and negative terminals of the PV cell. The short circuit current is directly proportional to the irradiance of the sunlight.

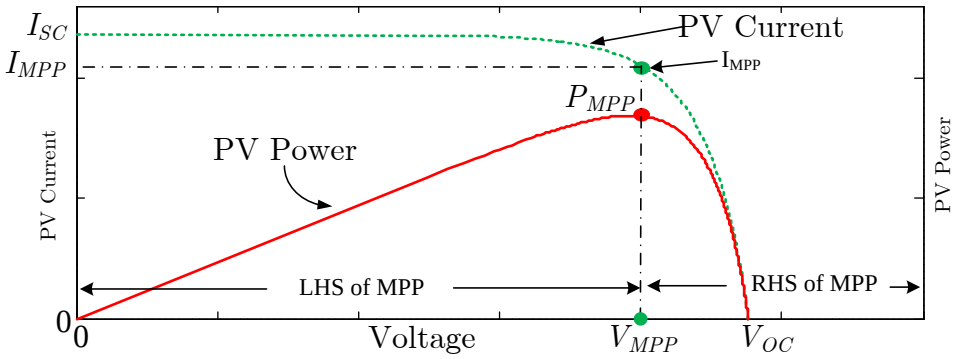

Figure 3.2: Typical characteristics of PV array.

Open Circuit Voltage (V_{oc}): Open circuit voltage is the maximum voltage that a PV cell can generate at the given weather conditions when the cell current is zero. This situation is possible in case of no load condition.

Maximum Power Point MPP: The operating point at which the PV cell generates the maximum power is MPP as shown in Fig. 3.2. The output power at MPP is given as

$$P_{MPP} = V_{MPP} * I_{MPP} \tag{3.1}$$

where V_{MPP} and I_{MPP} are voltage and currents at which maximum power occurs. This operating point is determined by choosing correct value of connected load.

Fill Factor (FF): The fill factor is an indicator of the quality of the PV cell. The sharpness of the knee in an I-V characteristics indicates how well a (p-n) junction is manufactured. The ideal value of the fill factor is unity. The maximum practical value of fill factor is 0.88. Fill factor is defined as the ratio of the maximum power generated at MPP to the maximum theoretical power.

$$FF = \frac{P_{max,practical}}{P_{max,theoretical}} = \frac{V_{MPP} * I_{MPP}}{V_{oc} * I_{sc}} \tag{3.2}$$

Efficiency of PV Cell: Only a small part of solar radiation incident on the PV cell is converted to electricity. The conversion efficiency of PV cell is defined as the "ratio

of electrical power generated to the amount of incident solar energy per second (P_{inc})". The equation of solar cell power conversion efficiency is given as

$$\eta = \frac{P_{MPP}}{P_{inc}} = \frac{V_{MPP} * I_{MPP}}{A_{cell} * S} \tag{3.3}$$

where A_{cell} is area of PV cell and S is irradiance.

3.3 Maximum Power Point Tracking Algorithms

The objective of the MPPT algorithms is to find automatically the voltage (V_{MPP}) or current (I_{MPP}) at which maximum power (P_{MPP}) can be generated from PV panel at the given temperature and the irradiance. Several MPPT algorithms are available in the literature. Most of these algorithms respond to both temperature and irradiance, but few of them are specifically more effective if temperature is considered as constant. Most of the algorithms respond normally even though the physical property of PV panel changed due to ageing, but few are open loop algorithms which require fine periodic tuning. The PV panel has non-linear I-V characteristics, which makes it difficult to supply certain loads. This problem can be solved to certain extent by using power converter devices between the source and load, especially DC/DC converters like boost converter whose duty ratio is controlled by MPPT algorithm. The following algorithms are some of the widely used MPPT algorithms applied on various PV applications [13].

3.3.1 Perturbation and Observation / Hill Climbing

Among the several MPPT algorithms, much focus has been on perturb and observe (P&O) methods. The P&O method involves a perturbation in the operating voltage (ΔV) of solar array and hill climbing involves a perturbation in the duty ratio of power converter. The flowchart of conventional P&O MPPT algorithm is shown in Fig. 3.3. In the flowchart the parameters $V(k)$, $I(k)$ and $P(k)$ are voltage, current and power of PV source at k^{th} instant respectively. The parameter (ΔV) is fixed perturbation size of the voltage. In P&O method the voltage is increased or decreased with a fixed step size in the direction of reaching the MPP as shown in Table. 3.1. This process is periodically

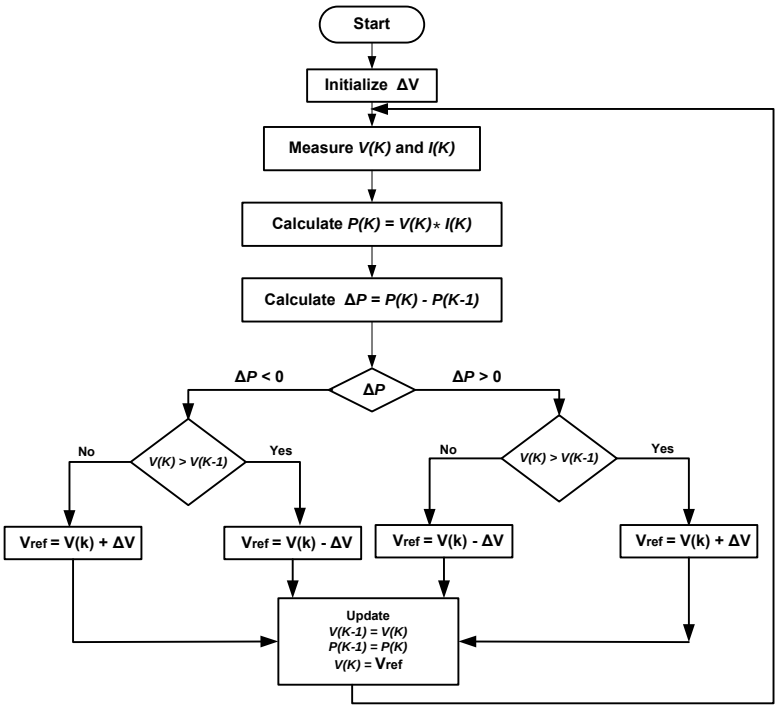

Figure 3.3: Flowchart of conventional P&O MPPT algorithm.

repeated until the MPP is reached. At steady state, the oscillations of operating point around the MPP gives rise to wastage of some available energy. These oscillations can be minimized by reducing the fixed step size, but it takes relatively more time to reach the MPP. The solution to this conflicting situation is to have a variable step size as suggested in [13]. Even though, implementation of these methods is simple, it is not very accurate and rapid, since the effects of irradiation and temperature are not taken into account. Different methods are proposed to address these issues by considering adaptive perturbation. The performance of P&O method is significantly depends on the trade off between the tracking speed and oscillations that occur around the MPP.

Perturbation	**Change in Power**	**Next Perturbation**
Positive	Positive	Positive
Positive	Negative	Negative
Negative	Positive	Negative
Negative	Negative	Positive

Table 3.1: Summary of P & O Method

3.3.2 Incremental Conductance

Incremental conductance (IC) is another MPP method, which is based on the fact that slope of the PV array power curve is zero at MPP, negative on the right side and positive on the left side of MPP. Mathematically, it can be given as

$$\begin{aligned} dP/dV &= 0 && \text{at MPP} \\ dP/dV &> 0 && \text{left of MPP} \\ dP/dV &< 0 && \text{right of MPP} \end{aligned} \tag{3.4}$$

where dP/dV is derivative of power with respect to voltage. As power is expressed as product of voltage and current, the derivative of power with respect to voltage can be expressed as

$$\frac{dP}{dV} = \frac{d(VI)}{dV} = I + V\frac{dI}{dV} \approx I + V\frac{\Delta I}{\Delta V} \tag{3.5}$$

where ΔI and ΔV are change in current and voltage respectively. Substituting (3.5) in (3.4) results into the following conditions

$$\begin{aligned} \Delta I/\Delta V &= -I/V && \text{at MPP} \\ \Delta I/\Delta V &> -I/V && \text{left of MPP} \\ \Delta I/\Delta V &< -I/V && \text{right of MPP} \end{aligned} \tag{3.6}$$

Therefore, the MPP can be tracked by comparing the instantaneous conductance (I/V) with the incremental conductance ($\Delta I/\Delta V$). The flowchart of the incremental conductance method is shown in Fig. 3.4. Incremental conductance method inherits the same problems as P&O, namely the trade off between the speed and oscillations. Different IC techniques are proposed to improve the performance, but during rapid fluctuations of irradiance and temperature the tracking speed reduces significantly.

3.3.3 Fractional Open Circuit Voltage

In this algorithm, the MPP voltage can be calculated from the empirical relationship as given below.

$$V_{MPP} \approx k_{oc} V_{OC} \tag{3.7}$$

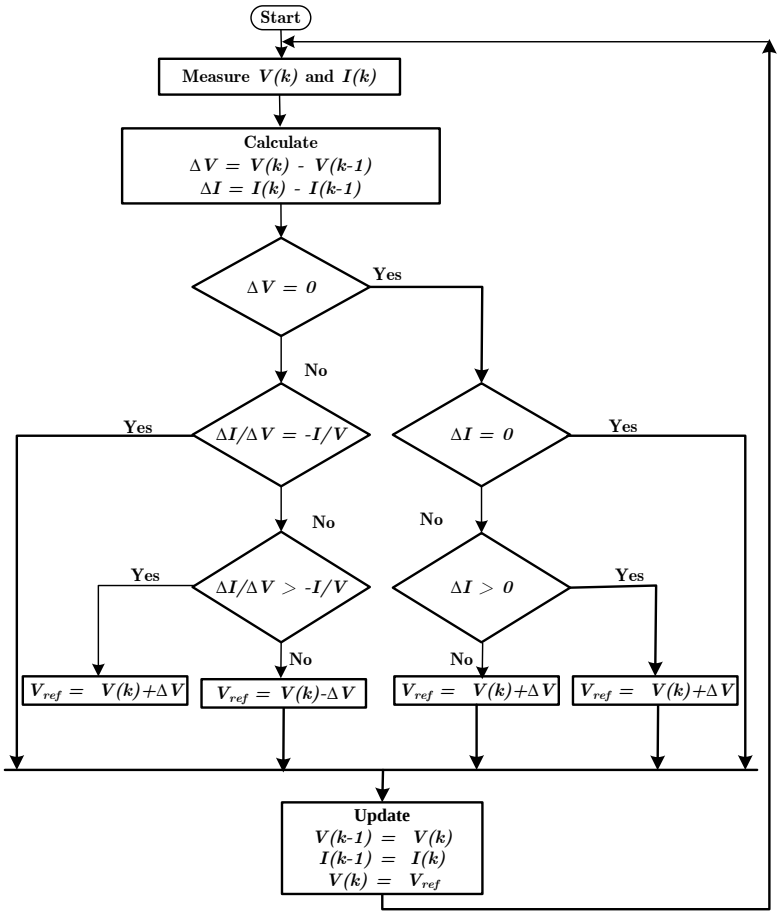

Figure 3.4: Flowchart of incremental conductance method.

where k_{oc} is a proportionality constant. The constant k_{oc} varies between 0.71 and 0.78 depending on the weather conditions. The value of k_{oc} can be finded out by analysing the PV system for different values of irradiance and temperatures. In this method, the open circuit voltage is measured by opening the PV system for fraction of seconds, and then the MPP voltage is calculated from equation (3.7). This process is repeated periodically by shutting down the power converter for fraction of seconds. Therefore, it results in temporary loss of power. Further, the PV system never operates at its MPP, since the V_{MPP} is an approximation. Even though this method is not accurate, it is very simple to implement and does not require any advanced digital signal processor or micro controller controls.

3.3.4 Fractional Short Circuit Current (FSCC)

It results from the fact that, under varying weather conditions, the MPP current is approximately linearly related to the short circuit current of the PV system as given in [13]. This is mathematically represented as

$$I_{MPP} \approx k_{sc} I_{SC} \tag{3.8}$$

where k_{sc} is a proportionality constant. Depending on the variation of irradiance and temperature, the constant k_{sc} varies between 0.78 and 0.92. The short circuit current is measured by shorting the PV system periodically. An additional switch is used to short the PV system, which increases the number of components and cost. The output power is further reduced during this period. Since this method approximates the constant ratio, its accuracy cannot be guaranteed under varying weather conditions.

3.4 Modelling of PV Module

Photovoltaic cells exhibits a non-linear I-V and P-V characteristics which vary with cell temperature (T) and solar irradiance (S). Different equivalent circuit models of PV cell have been discussed in the literature. In this work, a general single diode PV model is considered [13].

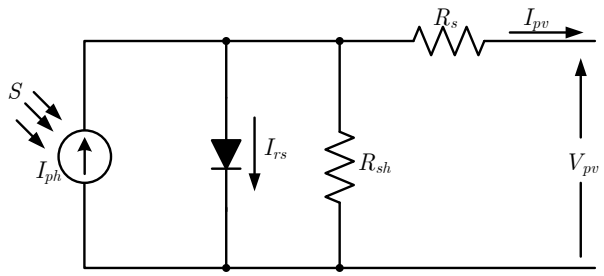

Figure 3.5: Equivalent circuit of PV Cell.

3.4.1 PV Cell

The equivalent circuit of the general model of PV cell, which consists of a photo current source, a parallel resistor representing a leakage current, a diode, and a series resistor serves as a internal resistance to the current flow is shown in Fig. 3.5. The non-linear voltage-current characteristic equation of he PV cell is given as

$$I_{pv} = I_{ph} - I_{rs}\left(e^{\frac{q(V_{pv}+I_{pv}R_s)}{A`kT}} - 1\right) - \frac{V_{pv} + I_{pv}R_s}{R_{sh}} \tag{3.9}$$

where

V_{pv}	terminal voltage (V)
I_{pv}	terminal current (A)
I_{ph}	light generated current or photo current (A)
I_{rs}	diode reverse saturation current
q	electron charge ($= 1.609$ x 10^{-19} C)
A	diode ideality constant
k	Boltzmann's constant ($= 1.38$ x 10^{-23} J/K)
T	cell absolute temperature (K)
R_s	series resistance (Ω)
R_{sh}	shunt resistance (Ω)

The photon current which depends on irradiance and temperature is given by

$$I_{ph} = \frac{S}{S_{nom}}\big(I_{sc} + \alpha_{sc}(T - T_{nom})\big) \tag{3.10}$$

where I_{sc} is short circuit current (A), α_{sc} is temperature coefficient of I_{sc} (A/^{o}C), S is solar irradiance (W/m^2), S_{nom} is irradiance at standard test condition (STC) and T_{nom} is cell temperature at STC.

The diode reverse saturation current varies as a cubic function of the temperature and it can be expressed as

$$I_{rs} = \frac{I_{SC}(T_{nom})}{\left(e^{\frac{qV_{OC}(T_{nom})}{AkT}} - 1\right)}\left(\frac{T}{T_{nom}}\right)^3 e^{\frac{qE_G}{Ak}\left(\frac{1}{T} - \frac{1}{T_{nom}}\right)} \tag{3.11}$$

where E_G is band-gap of the semiconductor cell (V).

To determine the unknown parameters of the PV model, number of approaches are described in literature. For modelling purposes, a simple mathematical approach has

been considered in this work, which depends on parameters given in the PV panel data sheet [13]. Using the details given in the data sheet, a system of equations are derived as given in equation (3.12) and solved for the five unknown parameters I_{ph}, I_{rs}, A, R_s and R_{sh}.

$$\begin{aligned} I_{oc} &= 0 = I_{ph} - I_{rs}\left(e^{\frac{qV_{OC}}{AkT}} - 1\right) - \frac{V_{OC}}{R_{sh}} \\ I_{MPP} &= I_{ph} - I_{rs}\left(e^{\frac{q(V_{MPP}+I_{MPP}R_s)}{AkT}} - 1\right) - \frac{V_{MPP}+I_{MPP}R_s}{R_{sh}} \\ I_{sc} &= I_{ph} - I_{rs}\left(e^{\frac{q(I_{sc}R_s)}{AkT}} - 1\right) - \frac{I_{sc}R_s}{R_{sh}} \\ \frac{dP_{pv}}{dV} &= 0 \qquad \text{at maximum power point} \\ \frac{dI}{dV} &= -\frac{1}{R_{sh}} \qquad \text{at} \quad I = I_{SC}, V = V_{OC} \end{aligned} \tag{3.12}$$

It is not possible to determine these parameters by direct substitution method, due to the non-linear nature of the equations. Therefore, numerical methods are used to solve these equations.

3.4.2 PV Panel

Due to low power ratings of each individual PV cell, the cells are connected in series-parallel configuration in order to produce required power. The equivalent circuit is shown in Fig. 3.6.

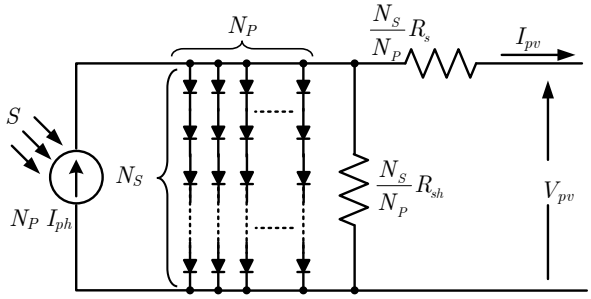

Figure 3.6: Equivalent circuit of PV Panel.

The PV panel is described by its non-linear I-V characteristic equation given as [13]

$$I_{pv} = N_p I_{ph} - N_p I_{rs}\left(e^{\frac{q(V_{pv}/N_s + I_{pv}R_s/N_p)}{AkT}} - 1\right) - \frac{N_p V_{pv}/N_s + I_{pv}R_s}{R_{sh}} \tag{3.13}$$

where N_s is number of cells connected in series and N_p is number of strings connected in parallel as shown in Fig. 3.6.

3.4.3 Solution for Non-linear Equation

The model is processed in a MATLAB script file. Newton Raphson (N-R) method is used to solve the non-linear equations as given [29]

$$x_{n+1} = x_n - \frac{f(x_n)}{f'(x_n)} \tag{3.14}$$

where x_n is the value of x at n^{th} instant, f' is the derivative of f with respect to x, and f can be derived from equation (3.13) is given as

$$f(x) = I_{pv} - N_p I_{ph} + \frac{N_p V_{pv}/N_s + I_{pv} R_s}{R_{sh}} + N_p I_{rs}\left(e^{\frac{q(V_{pv}/N_s + I_{pv} R_s/N_p)}{AkT}} - 1\right) \tag{3.15}$$

where x can be either I_{pv} or V_{pv}.

3.5 Characteristics of PV Panel

The electrical characteristics of the PV cell mainly depends on the irradiance and temperature of the cell. The I-V and P-V characteristic curves represents all the possible current, power and voltage operating points for the PV panel. Using the equations in (3.12) the five unknown parameters I_{ph}, I_{rs}, A, R_s and R_{sh} are solved as explained in [13]. These values are substituted in equation (3.15) to obtain I-V and P-V characteristics. These characteristics are obtained by solving equation (3.15) for I_{pv} by varying V_{pv} from zero to open circuit voltage for the given irradiance and cell temperature. Typical characteristics of PV panel for different values of irradiance and cell temperature are drawn as shown in Fig. 3.7 and in Fig. 3.8. Fig. 3.7 shows the characteristics of PV panel for different values of irradiance ($S_1 > S_2 > S_3$) at constant cell temperature. Similarly, Fig. 3.8 shows the characteristics of PV panel for different values of cell temperature ($T_1 > T_2 > T_3$) at constant irradiance.

The I-V characteristic of the PV panel tells that there are two regions in the curve: one is voltage source region and the other is current source region. In the voltage source region (i.e., in the right hand side of the curve), the internal impedance is low and in the current source region (i.e., in the left hand side of the curve), the impedance is high. Therefore, the cell operates as a constant voltage source at low values of current, and as a constant current source at low values of voltage. The operating point of PV panel in the I-V curve is determined by the load connected to it. The optimum electrical load is the load at which PV panel operates at its MPP.

3.5.1 Effect of Irradiance

The characteristics of the PV panel are highly dependent on the solar irradiation levels. The irradiance continuously changes with the environmental conditions. However, technology is available to track these changes and operate the PV panel at MPP. When solar irradiance reduces, the photon flux reaching the PV panel reduces. It results in less generation of photon current. As shown in Fig. 3.7 the changes in irradiance slightly

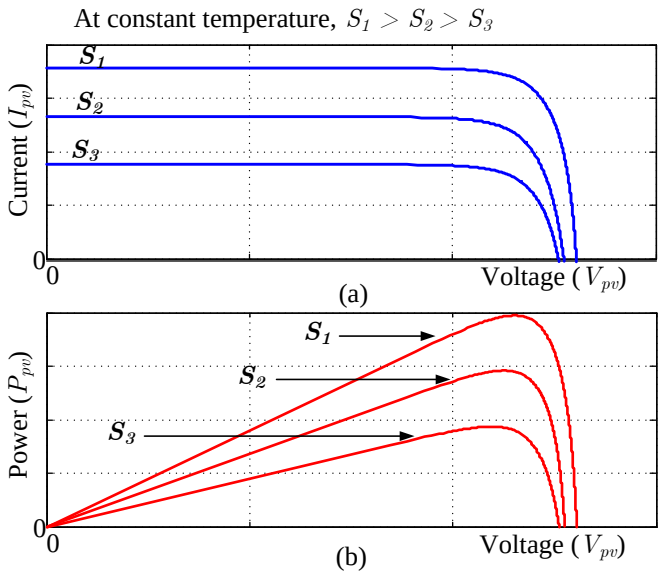

Figure 3.7: Effect of irradiance variation at constant temperature: (a) I-V characteristics (b) P-V characteristics.

effects the open circuit voltage and it is almost negligible. Its most significant effect is

on short circuit current which is directly proportional to the solar irradiance. Thus, for the same operating voltage, the current increases with increase in irradiance, and hence the output power.

3.5.2 Effect of Temperature

On contrary to the effect of irradiance on power, the increase in temperature has a negative impact on the power generation capability of the PV panel. The output current decrease with increase in temperature. This is due to the decrease in mobility of charge carriers in the semiconductor material. Another reason is increase of band gap energy due to increase in temperature. More energy is required to cross the forbidden energy gap by the electrons due to increased band gap, thus only few electrons can cross it. Therefore, the output current and power are reduced. Fig. 3.8 shows that at constant irradiance, any change in the temperature has a significant effect on the open circuit voltage, while negligible effect on the short circuit current.

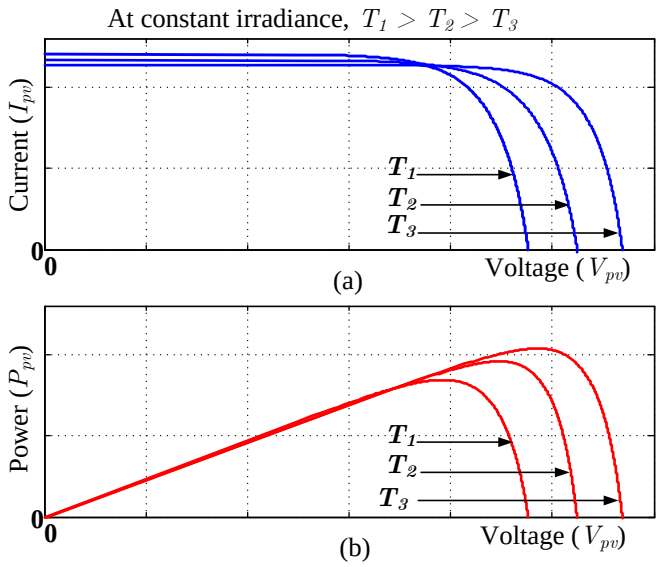

Figure 3.8: Effect of temperature variation at constant irradiance: (a) I-V characteristics (b) P-V characteristics.

3.6 Summary

In this chapter, various parameters of pv cell, different MPPT algorithms for PV systems, modelling of PV cell and PV panel are discussed. Out of several equivalent circuit models of PV cell, a general single diode PV model is considered. Further, the I-V and P-V are studied for different weather conditions.

CHAPTER 4

DUAL VSI TOPOLOGY WITH POWER QUALITY IMPROVEMENT FEATURES

In microgrid, power from different renewable energy sources such as photo voltaic (PV) systems, wind energy systems, fuel cells are interfaced to grid and loads using power electronic converters. A grid interactive inverter plays an important role in exchanging power from microgrid to the grid and the connected load. The microgrid inverter can either work in a grid sharing mode while supplying a part of local load or in grid injecting mode, by injecting power to main grid. Maintaining power quality is another important aspect which has to be addressed while connecting microgrid with utility grid. When a grid connected inverter is used for active power injection as well as for load compensation, the inverter capacity that can be utilized for load compensation is decided by the available instantaneous microgrid real power. In most of the renewable based DG units, the real power generation is highly fluctuating. Considering the case of grid connected PV inverter, the available capacity of the inverter to supply the reactive power becomes less during the maximum solar insolation periods. However, the reactive power to regulate the PCC voltage is very much needed during this period [14]. It indicates that, providing multi-functionalities in a single inverter degrades either the real power injection or the load compensation capabilities.

This chapter describes and demonstrates a dual voltage source inverter (DVSI) scheme in which, the power generated by the microgrid is injected as real power by the main voltage source inverter (MVSI) and the reactive, harmonic and unbalanced load compensation is performed by auxiliary voltage source inverter (AVSI). This scheme has an advantage that the rated capacity of MVSI can always be used to inject real power to grid, if sufficient renewable power is available at the dc link. In DVSI scheme, as total load power is supplied by two inverters, power losses across the semiconductor switches of each inverter is reduced. This increases its reliability as compared to a single inverter with multifunctional capabilities. Also, smaller size modular inverters can

operate at high switching frequencies with a reduced size of interfacing inductor and the reduction in filter cost. Moreover, as main inverter is supplying real power, the inverter has to track the fundamental positive sequence of current. This reduces the bandwidth requirement of the main inverter. The inverters in the proposed scheme use two separate dc links which increases the flexibility of operation. Since, the auxiliary inverter is supplying zero sequence of load current, a three-phase three-leg inverter topology with a single dc storage capacitor can be used for main inverter. This in turn reduces the dc-link voltage requirement of the main inverter. Thus, the use of two separate inverters in the proposed DVSI scheme provides, increased reliability, better utilization of microgrid power, reduced dc-link voltage rating, less bandwidth requirement of main inverter, and reduced filter size [14].

Control algorithms are developed based on instantaneous symmetrical component theory (ISCT) to operate DVSI in grid connected mode, while considering non-stiff grid voltage [9],[14]. The extraction of fundamental positive sequence of PCC voltage is done by using dq0 transformation [11]. The control strategy is tested with two voltage source inverters connected to a three-phase four-wire distribution system. Effectiveness of the control algorithm is validated through detailed simulation results.

4.1 DVSI Topology

The power circuit of the DVSI topology is shown in Fig. 4.1. It consists of a neutral point clamped (NPC) inverter to realize AVSI and a three leg inverter for MVSI. These are connected to grid at the PCC and supplies non-linear and unbalanced load. The function of the AVSI is to compensate the unbalance, reactive and harmonic components in the load currents. Here, load currents in three phases are represented by i_{la}, i_{lb} and i_{lc} respectively. Also, $i_{g(abc)}$, $i_{\mu gm(abc)}$ and $i_{\mu gx(abc)}$ represent grid currents, MVSI currents and AVSI currents in three phases respectively. The dc link of the AVSI utilizes a split capacitor topology, with two capacitors C1 and C2.

The MVSI delivers the available power at the distributed energy resource (DER) to the grid. The DER can be a dc source or an ac source with rectifier coupled to dc link. Usually, renewable sources like fuel cell and photovoltaic energy sources generate

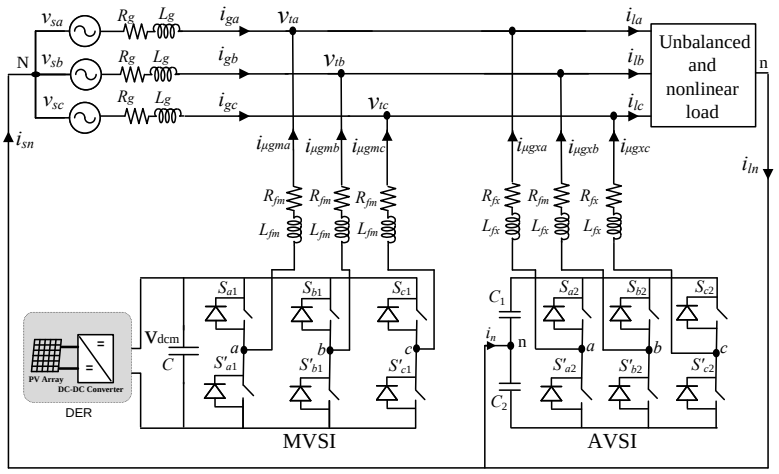

Figure 4.1: Topology of DVSI scheme.

power at variable low dc voltage, while the variable speed wind turbines generate power at variable ac voltage. Therefore, the power generated from these sources uses a power conditioning stage before it is connected to the input of MVSI. In this study, DER is the dc source formulated by PV array through a dc-dc converter. To eliminate the high frequency switching components generated due to the switching of power electronic switches in the inverters, an inductor filter is used. The system considered in this study is assumed to have some amount of feeder resistance Rg, and inductance Lg. Due to the presence of this feeder impedance, PCC voltages are affected with harmonics. The extraction of fundamental positive sequence of PCC voltages and control strategy for the reference current generation of two inverters in DVSI scheme are detailed in the further sections.

4.1.1 Design of DVSI Parameters

The design of various parameters of AVSI and MVSI are discussed in the following [14], [15], [16].

A. Auxiliary Voltage Source Inverter (AVSI)

The important parameters of AVSI like, dc link voltage (V_{dc}), dc storage capacitor

(C_1 and C_2), interfacing inductance (L_{fx}), and hysteresis band ($\pm h_x$) are selected based on the design method of split capacitor DSTATCOM topology. The dc link voltage across each capacitor is taken as 1.6 times the peak of phase voltage. The total dc-link voltage reference (V_{dcref}) is found to be 1040 V.

The dc capacitor values of AVSI are chosen based on the change in dc-link voltage during transients. Let the total load rating be S kVA. In the worst case, the load power may vary from minimum to maximum i.e., from 0 to S kVA. AVSI needs to exchange real power during transient to maintain the load power demand. This transfer of real power during the transient will result in deviation of capacitor voltage from its reference value. Assume that the voltage controller takes n cycles i.e., nT seconds to act, where T is the time period of system voltage. Hence, maximum energy exchange by AVSI during transient will be nST. This energy will be equal to change in the capacitor stored energy. Therefore,

$$\frac{1}{2}C_1\left(V_{dcr}^2 - V_{dc1}^2\right) = nST \tag{4.1}$$

where V_{dcr} and V_{dc1} are the reference dc voltage and maximum permissible dc voltage across C_1 during transient respectively. Here $S = 5kVA$, $V_{dcr} = 520$ V, $V_{dc1} = 0.8 * V_{dcr}$ or $1.2 * V_{dcr}$, $n = 1$ and $T = 0.02$ s. Substituting these values in (4.1), the dc-link capacitance (C_1) is calculated to be 2000 mF:

The interfacing inductance is given by

$$L_{fx}\frac{1.6V_m}{4h_x f_{max}} \tag{4.2}$$

Assuming a maximum switching frequency (f_{max}) of 10 kHz and hysteresis band (h_x) as 5% of load current (0.5 A), the value of L_{fx} is calculated to be 26 mH.

B. Main Voltage Source Inverter (MVSI)

The MVSI uses a three leg inverter topology. Its dc link voltage is obtained as $1.15 * V_{ml}$, where V_{ml} is the peak value of line voltage. This is calculated to be 648 V. Also, MVSI supplies a balanced sinusoidal current at unity power factor. Therefore, zero sequence switching harmonics will be absent in the output current of MVSI. This

reduces the filter requirement for MVSI as compared to AVSI. In this analysis, a filter inductance (L_{fm}) of 5 mH is used.

4.1.2 Advantages of DVSI

The various advantages of the proposed DVSI scheme over a single inverter scheme with multifunctional capabilities [14],[16] are discussed here as follows.

1. **Increased reliability:** DVSI scheme has increased reliability, due to the reduction in failure rate of components and the decrease in system down time cost. In this scheme, the total load current is shared between AVSI and MVSI. This reduces the individual switch current and hence the power losses. The lower heat dissipation due to reduced power losses across switches in turn decreases the failure rate of inverter switches. Moreover, if one inverter fails, the other unit continues its operation. This reduces the outage and hence the down time cost. The system down time cost includes the repairing cost as well as the cost of lost energy which could be otherwise supplied during the down time of the system. The reduction in system down time cost improves the reliability.

2. **Reduction in filter size:** In DVSI scheme, the current supplied by each inverter is reduced and hence the current rating of individual filter inductor reduces. This reduction in current rating reduces the filter size. Also, in this scheme, hysteresis current control is used to track the inverter reference currents. As given in equation (4.2), the filter inductance is decided by the inverter switching frequency. Since the lower current rated semiconductor device can be switched at higher switching frequency, the inductance of the filter can be lowered. This decrease in inductance further reduces the filter size.

3. **Improved flexibility:** Both the inverters are fed from separate dc-links which allows them to operate independently, thus increasing the flexibility of the system. For instance, if the dc-link of the main inverter is disconnected from the system, the load compensation capability of the auxiliary inverter can still be utilized.

4. **Better utilisation of microgrid power:** DVSI scheme helps to utilize full ca-

pacity of MVSI to transfer the entire power generated by DG units as real power to ac bus, as there is AVSI for harmonic and reactive power compensation. This increases the active power injection capability of DGs in microgrid.

5. **Reduced dc-link voltage rating:** Since the main inverter is not delivering any zero sequence load current components, a single capacitor three-leg VSI topology can be used. Therefore the dc-link voltage rating of MVSI is reduced as compared to single inverter system. The reduction in dc-link voltage is explained as follows.

The dc link voltage of AVSI is selected to achieve good tracking performance. In the DVSI scheme, AVSI uses a split capacitor VSI topology. The total dc link of AVSI is obtained as $2 * 1.6V_m$, where V_m is the peak value of phase voltage. This is calculated to be 1040 V. The MVSI uses a three leg VSI topology. Its dc link voltage is obtained as $1.15 * V_{ml}$, where V_{ml} is the peak value of line voltage. This is calculated to be 648 V. Thus in DVSI scheme, the DG power available at the dc link of MVSI can be at 650 V. If a single inverter is used to supply an unbalanced non-linear load using a split capacitor VSI topology, the microgrid power available at the dc link must be at 1040 V. Therefore, the reduction in dc link voltage of MVSI is approximately 38%.

4.2 CONTROL STRATEGY OF DVSI SCHEME

4.2.1 Performance During Adverse Voltage Conditions

The propagation of unbalanced and non-linear load current through the feeder impedance of distribution system makes the PCC voltages unbalanced and distorted. However, the control algorithm for reference current generation using ISCT requires balanced sinusoidal PCC voltages. Therefore, the fundamental positive sequence components of the PCC voltages are to be extracted for the reference current generation [11]. In this work, $dq0$ transformation is used to extract the balanced sinusoidal voltages from unbalanced and distorted PCC voltages. The PCC voltages in natural reference frame, $v_{t(abc)}$ are first transformed into $dq0$ reference frame using the equation

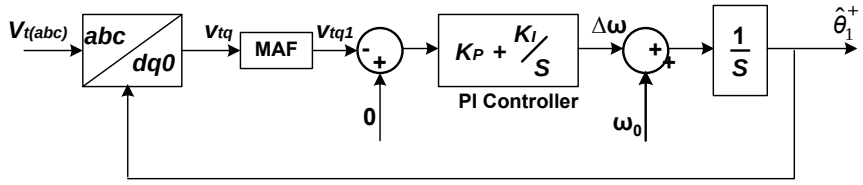

Figure 4.2: Schematic diagram of PLL..

$$\begin{bmatrix} v_{td} \\ v_{tq} \\ v_{t0} \end{bmatrix} = C \begin{bmatrix} v_{ta} \\ v_{tb} \\ v_{tc} \end{bmatrix} \tag{4.3}$$

where

$$C = \sqrt{\frac{2}{3}} \begin{bmatrix} \sin\hat{\theta}_1^+ & \sin(\hat{\theta}_1^+ - 120^\circ) & \sin(\hat{\theta}_1^+ + 120^\circ) \\ \cos\hat{\theta}_1^+ & \cos(\hat{\theta}_1^+ - 120^\circ) & \cos(\hat{\theta}_1^+ + 120^\circ) \\ \frac{1}{\sqrt{2}} & \frac{1}{\sqrt{2}} & \frac{1}{\sqrt{2}} \end{bmatrix} \tag{4.4}$$

and θ_1^+ is the estimated phase of PCC voltage using the PLL shown in Fig. 4.2. Since the PCC voltages are unbalanced and distorted, the transformed voltages in dq0 frame (v_{td} and v_{tq}) contain average and oscillating components of voltages. These can be represented as

$$v_{td} = \overline{v}_{td} + \widetilde{v}_{td}, v_{tq} = \overline{v}_{tq} + \widetilde{v}_{tq} \tag{4.5}$$

where $\overline{v}_{td}$ and $\overline{v}_{tq}$ represent the average components of v_{td} and v_{tq} respectively. The terms, $\widetilde{v}_{td}$ and $\widetilde{v}_{tq}$ indicate the oscillating components of v_{td} and v_{tq} respectively. Now the fundamental positive sequence of PCC voltages in natural reference frame can be obtained with the help of inverse $dq0$ transformation as given by

$$\begin{bmatrix} v_{ta1}^+ \\ v_{tb1}^+ \\ v_{tc1}^+ \end{bmatrix} = C^T \begin{bmatrix} \overline{v}_{td} \\ \overline{v}_{tq} \\ 0 \end{bmatrix} \tag{4.6}$$

These voltages v_{ta1}^+, v_{tb1}^+ and v_{tc1}^+ are used in the reference current generation algorithms, so as to draw balanced sinusoidal currents from the source.

An accurate detection of voltage phase, $\hat{\theta}_1^+$ is required to extract the fundamental positive sequence components of voltages using $dq0$ transformation. A modified synchronous reference frame (SRF) based phase locked loop (PLL) [16] is used in this work to get $\hat{\theta}_1^+$. The schematic diagram of this PLL is shown in Fig. 4.2. It mainly consists of a PI controller and an integrator. In this PLL, the MAF output of SRF terminal voltage in q-axis (v_{tq1}) is compared with 0 voltage and error voltage thus obtained is given to the PI controller. The frequency deviation $\Delta\omega$ from the PI controller is then added to the reference frequency ω_0 and fed to the integrator to get $\hat{\theta}_1^+$. It can be proved that, when $\hat{\theta}_1^+ = \omega_0 t$, the fundamental positive sequence of q axis voltage in $dq0$ frame v_{tq1}^+ becomes zero and hence the PLL is locked to $\hat{\theta}_1^+$.

The unbalanced and distorted PCC voltages are expressed in terms of their positive and negative sequence components as follows.

$$\begin{aligned} v_{ta}(t) &= \sum_{h=1}^{\infty} \sqrt{2}\big(V_h^+ \sin\theta_h^+ + V_h^- \sin\theta_h^-\big) \\ v_{tb}(t) &= \sum_{h=1}^{\infty} \sqrt{2}\bigg(V_h^+ \sin(\theta_h^+ - \frac{2\pi}{3}) + V_h^- \sin(\theta_h^- + \frac{2\pi}{3})\bigg) \\ v_{tc}(t) &= \sum_{h=1}^{\infty} \sqrt{2}\bigg(V_h^+ (\sin\theta_h^+ + \frac{2\pi}{3}) + V_h^- (\sin\theta_h^- - \frac{2\pi}{3})\bigg) \end{aligned} \tag{4.7}$$

These voltages in natural reference frame are transformed to $dq0$ frame using equation (4.3). The transformed voltages in q-axis is obtained as

$$v_{tq}(t) = \sum_{h=1}^{\infty} \sqrt{3}\bigg(V_h^+ (\sin\theta_h^+ - \hat{\theta}_1^+) - V_h^- (\sin\theta_h^- + \hat{\theta}_1^+)\bigg) \tag{4.8}$$

This q-axis voltage is given to a MAF with a window of one fundamental time period ($\omega_0 t = \theta_1^+$). The output voltage from this MAF is given by

$$\begin{aligned} v_{tq1}(t) &= \sqrt{3}V_1^+ (\sin\theta_1^+ - \hat{\theta}_1^+) - \sqrt{3}V_1^- (\sin\theta_1^- + \hat{\theta}_1^+) \\ &= v_{tq1}^+ + v_{tq1}^- \end{aligned} \tag{4.9}$$

Using equation (4.9), when $\omega_0 t = \theta_1^+ = \hat{\theta}_1^+$ the component v_{tq1}^+ will be zero. On the one hand, if v_{tq1} is made equal to zero in the PLL, the PLL output will be locked to θ_1^+. Therefore, the PLL gives the fundamental frequency (ω_0) of PCC voltages even under unbalanced and distorted voltage conditions.

4.2.2 Reference Current Generation Algorithm

ISCT was developed primarily for unbalanced and non-linear load compensations by active power filters. The ISCT for load compensation is derived based on the following three conditions.

1. The source neutral current must be zero. Therefore,

$$i_{sa} + i_{sb} + i_{sc} = 0. \tag{4.10}$$

2. The phase angle between the fundamental positive sequence voltage (v^+_{ta1}) and source current (i_{sa}) is ϕ.

$$\angle v^+_{ta1} = \angle i_{sa} + \phi. \tag{4.11}$$

3. The average real power of the load (P_l) should be supplied by the source.

$$v^+_{ta1} i_{sa} + v^+_{tb1} i_{sb} + v^+_{tc1} i_{sc} = P_l. \tag{4.12}$$

Solving the above three equations, the reference source currents can be obtained as

$$\begin{aligned}
i^*_{sa} &= \left(\frac{v^+_{ta1} + \gamma^+ (v^+_{tb1} - v^+_{tc1})}{\sum_{j=a,b,c} {v^+_{tj}}^2} \right) P_l \\
i^*_{sb} &= \left(\frac{v^+_{tb1} + \gamma^+ (v^+_{tc1} - v^+_{ta1})}{\sum_{j=a,b,c} {v^+_{tj}}^2} \right) P_l \\
i^*_{sc} &= \left(\frac{v^+_{tc1} + \gamma^+ (v^+_{ta1} - v^+_{tb1})}{\sum_{j=a,b,c} {v^+_{tj}}^2} \right) P_l
\end{aligned} \tag{4.13}$$

where $\gamma = \tan \phi^+ / \sqrt{3}$. The term, ϕ is the desired phase angle between the fundamental positive sequence of PCC voltage and source current. To achieve unity power factor for source current, substitute $\gamma = 0$ in equation (4.13). Thus, the reference source currents for three phases are given by

$$i^*_{s(abc)} = \left(\frac{v^+_{t(abc)1}}{\sum_{j=a,b,c} {v^+_{tj}}^2} \right) P_l. \tag{4.14}$$

where i^*_{sa}, i^*_{sb} and i^*_{sc} are fundamental positive sequence of load currents drawn from the source, when it is supplying an average load power (P_l). The power, P_l , can be

computed using a moving average filter with a window of one cycle data points using equation (4.15)

$$P_l = \frac{1}{T}\int_{t_1-T}^{t_1}(v_{ta1}^{+}i_{la} + v_{tb1}^{+}i_{lb} + v_{tc1}^{+}i_{lc})dt \tag{4.15}$$

where t_1 is any arbitrary time instant. Finally, the reference currents for the compensator can be generated from the following.

$$i_{f(abc)}^{*} = i_{l(abc)} - i_{s(abc)}^{*} \tag{4.16}$$

Equation (4.16) can be used to generate the reference filter currents using ISCT, when the entire load active power, P_l, is supplied by the source and load compensation is performed by a single inverter. A modification in the control algorithm is required, when it is used for DVSI scheme. The following section discusses the formulation of control algorithm for DVSI scheme. The source currents, $i_{s(abc)}$ and filter currents, $i_{f(abc)}$ will be equivalently represented as grid currents, $i_{g(abc)}$ and AVSI currents, $i_{\mu gx(abc)}$ respectively in further sections. Control strategy of DVSI is developed in such a way that, grid and MVSI together share the active load power, and AVSI supplies rest of the power components demanded by the load.

A. Reference Current Generation for Auxiliary Inverter

The dc link voltage of the AVSI should be maintained constant for proper operation of the auxiliary inverter. The dc link voltage variation occurs in auxiliary inverter due to its switching and ohmic losses. These losses termed as P_{loss}, should also be supplied by the grid. An expression for P_{loss} is derived on the condition that, average dc capacitor current is zero to maintain a constant capacitor voltage [8]. The deviation of average capacitor current from zero will reflect as a change in capacitor voltage from a steady state value. A proportional integral (PI) controller is used to generate P_{loss} term as given by

$$P_{loss} = K_{Pv}e_{vdc} + K_{Iv}\int e_{vdc}dt \tag{4.17}$$

where $e_{vdc} = V_{dcref} - v_{dc}$, v_{dc} represents the actual voltage sensed and updated once in a cycle. In above equation, K_{Pv} and K_{Iv} represent the proportional and integral gains of dc link PI controller respectively. The P_{loss} term, thus obtained should be supplied

by the grid, and therefore AVSI reference currents can be obtained as given in equation (4.18). Here, the dc link voltage PI controller gains are so selected as to ensure stability and better dynamic response during load change.

$$
\begin{aligned}
i^*_{\mu gxa} &= i_{la} - \left(\frac{v^+_{ta1}}{\sum_{j=a,b,c} v^{+2}_{tj}}\right)(P_l + P_{loss}) \\
i^*_{\mu gxb} &= i_{lb} - \left(\frac{v^+_{tb1}}{\sum_{j=a,b,c} v^{+2}_{tj}}\right)(P_l + P_{loss}) \\
i^*_{\mu gxc} &= i_{lc} - \left(\frac{v^+_{tc1}}{\sum_{j=a,b,c} v^{+2}_{tj}}\right)(P_l + P_{loss})
\end{aligned}
\tag{4.18}
$$

B. Reference Current Generation for Main Inverter

The MVSI supplies balanced sinusoidal currents based on the available renewable power at DER. If MVSI losses are neglected, the power injected to grid will be equal to that available at DER ($P_{\mu g}$). The following equation, which is derived from ISCT can be used to generate MVSI reference currents for three phases (a, b and c).

$$
i^*_{\mu gm(abc)} = \left(\frac{v^+_{t(abc)1}}{\sum_{j=a,b,c} v^{+2}_{tj}}\right) P_{\mu g} \tag{4.19}
$$

where $P_{\mu g}$ is the available power at the dc link of MVSI.

The reference currents obtained from equations (4.18) and (4.19) are tracked by using hysteresis band current controller (HBCC). HBCC schemes are based on a feedback loop, usually with a two level comparator. This controller has the advantage of peak current limiting capacity, good dynamic response and simplicity in implementation [14]. A hysteresis controller is a high gain proportional controller. This controller adds certain phase lag in the operation based on the hysteresis band and will not make the system unstable. Also, the proposed DVSI scheme uses a first order inductor filter which retains the closed loop system stability. The entire control strategy is schematically represented in Fig. 4.3

Applying Kirchoff's current law (KCL) at the PCC in Fig. 4.3

$$
i^*_{\mu gxj} = i_{lj} - (i_{gj} + i_{\mu gmj}), j = a, b, c \tag{4.20}
$$

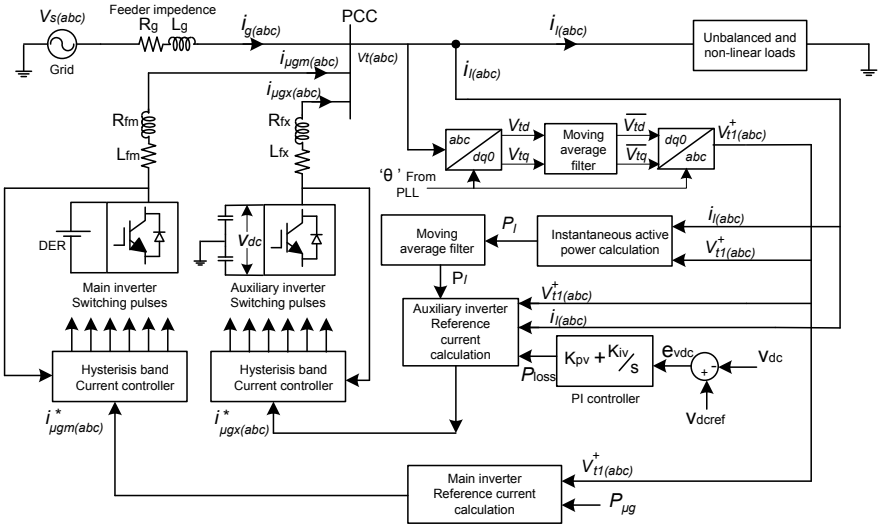

Figure 4.3: Schematic diagram showing the control strategy of DVSI scheme

By using equations (4.18) and (4.19), an expression for reference grid current in phase-a (i^*_{ga}) can be obtained as

$$i^*_{ga} = \left(\frac{v^+_{ta1}}{\sum_{j=a,b,c} v^{+2}_{tj}} \right) \left[(P_l + P_{loss}) - P_{\mu g} \right] \tag{4.21}$$

It can be observed that, if the quantity $(P_l + P_{loss})$ is greater than $P_{\mu g}$, the term $[(P_l + P_{loss}) - P_{\mu g}]$ will be a positive quantity, and i^*_{ga} will be in phase with v^+_{ta1}. This operation can be called as the grid supporting or grid sharing mode, as the total load power demand is shared between main inverter and grid. The term, P_{loss} is usually very small compared to P_l. On the other hand, if $(P_l + P_{loss})$ is less than $P_{\mu g}$, then $[(P_l + P_{loss}) - P_{\mu g}]$ will be a negative quantity, and hence i^*_{ga} will be in phase opposition with v^+_{ta1}. This mode of operation is called the grid injecting mode, as the excess power is injected to the grid.

4.3 SIMULATION RESULTS

The simulation model of DVSI scheme as shown in Fig. 4.1 is developed in MATLAB simulink to evaluate the performance. The simulation parameters of the system are

given in Table. 4.1. The simulation study demonstrates the grid sharing mode operation of DVSI scheme in steady state as well as in transient conditions.

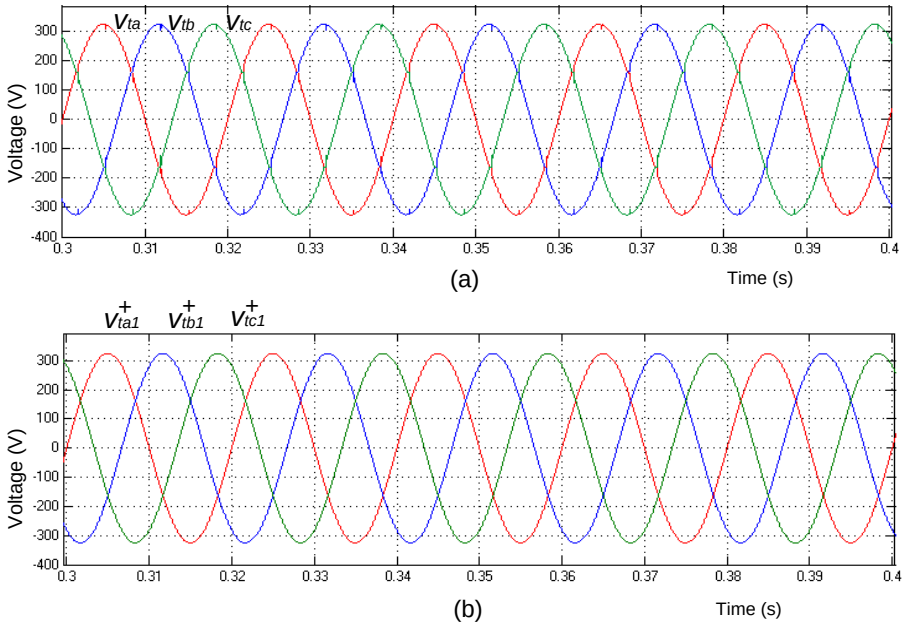

Figure 4.4: Without DVSI scheme: (a) PCC voltages and (b) Fundamental positive sequence of PCC voltages

The distorted PCC voltages due to the feeder impedance without DVSI scheme are shown in Fig. 4.4 (a). If these distorted voltages are used for the reference current generation of AVSI, the current compensation will not be proper. Therefore, the fundamental positive sequence of voltages are extracted from these distorted voltages using the algorithm explained in Section 4.2.1. These extracted voltages are given in Fig. 4.4 (b). These voltages are further used for the generation of inverter reference currents.

Fig. 4.5 (a)-(d) represents active power demanded by load (P_l), active power supplied by grid (P_g), active power supplied by MVSI ($P_{\mu g}$) and active power supplied by AVSI (P_x) respectively. It can be observed that, until t = 0.35 s, MVSI is generating 2.7 kW power and the load demand is 4.3 kW. Therefore, the remaining load active power 1.6 kW is drawn from the grid. At t = 0.35 s, the microgrid power is decreased to 1.1 kW. As the load demand is 4.3 kW, The remaining load active power 3.2 kw is drawn from the grid. In both the time periods, the microgrid is operating in grid sharing mode. One can also operate the microgrid in grid injecting mode if microgrid power is more

Parameters	Values
Grid Voltage	400 V (L-L), 50 Hz
Feeder impedance	$R_g = 0.5\ \Omega$, $L_g = 1.0mH$
AVSI	$C_1 = C_2 = 2200\ \mu F$, $V_{dcref} = 1040$V Interfacing inductor, $L_{fx} = 20mH$ Interfacing resistance $R_{fx} = 0.25\ \Omega$ Hysteresis band $(h_x) = 0.1$A
MVSI	Dc-link voltage, $V_{dcm} = 650$V Interfacing inductor, $L_{fm} = 5mH$ Interfacing resistance $R_{fm} = 0.25\ \Omega$ Hysteresis band $(\pm h_m) = 0.1$A
Unbalanced linear load	Z_{la} = 65+j25 Ω Z_{la} = 40+j15 Ω Z_{la} = 52+j18 Ω
Nonlinear load	$R = 200\ \Omega$
DC voltage controller gains	$K_{Pv} = 10$, $K_{Iv} = 0.05$

Table 4.1: System Parameters for Simulation Study of DVSI Scheme

than the load active power. Fig. 4.6 (a)-(c) shows the load reactive power (Q_l), reactive power supplied by AVSI (Q_x) and reactive power supplied by MVSI ($Q_{\mu g}$) respectively. It shows that, total load reactive power is supplied by AVSI, as expected.

Fig. 4.7 (a)-(d) shows the plots of load currents ($i_{l(abc)}$), currents drawn from grid ($i_{g(abc)}$), currents drawn from MVSI ($i_{\mu g(abc)}$), and currents drawn from the AVSI ($i_{\mu x(abc)}$) respectively. The load currents are unbalanced and distorted. The MVSI supplies a balanced and sinusoidal currents during grid supporting mode. The currents drawn from grid are also perfectly balanced and sinusoidal, as the auxiliary inverter compensates the unbalance and harmonics in load currents.

Fig. 4.8 (a) shows the plot of fundamental positive sequence of PCC voltage (v_{ta1}^{+}) and grid current in phase-a (i_{ga}) in grid sharing mode. From Fig. 4.8 (a) , one can observe that, when microgrid power decreases at $t = 0.35s$ the grid current drawn gets increases. Fig. 4.8 (b) establishes that, MVSI current in phase-a is always in phase with fundamental positive sequence of phase-a PCC voltage. The same is true for other two phases. Thus the compensation capability of AVSI makes the source current and MVSI current at unity power factor operation. The dc link voltage of AVSI is shown in Fig. 4.9. It indicates that the voltage is maintained constant at a reference voltage

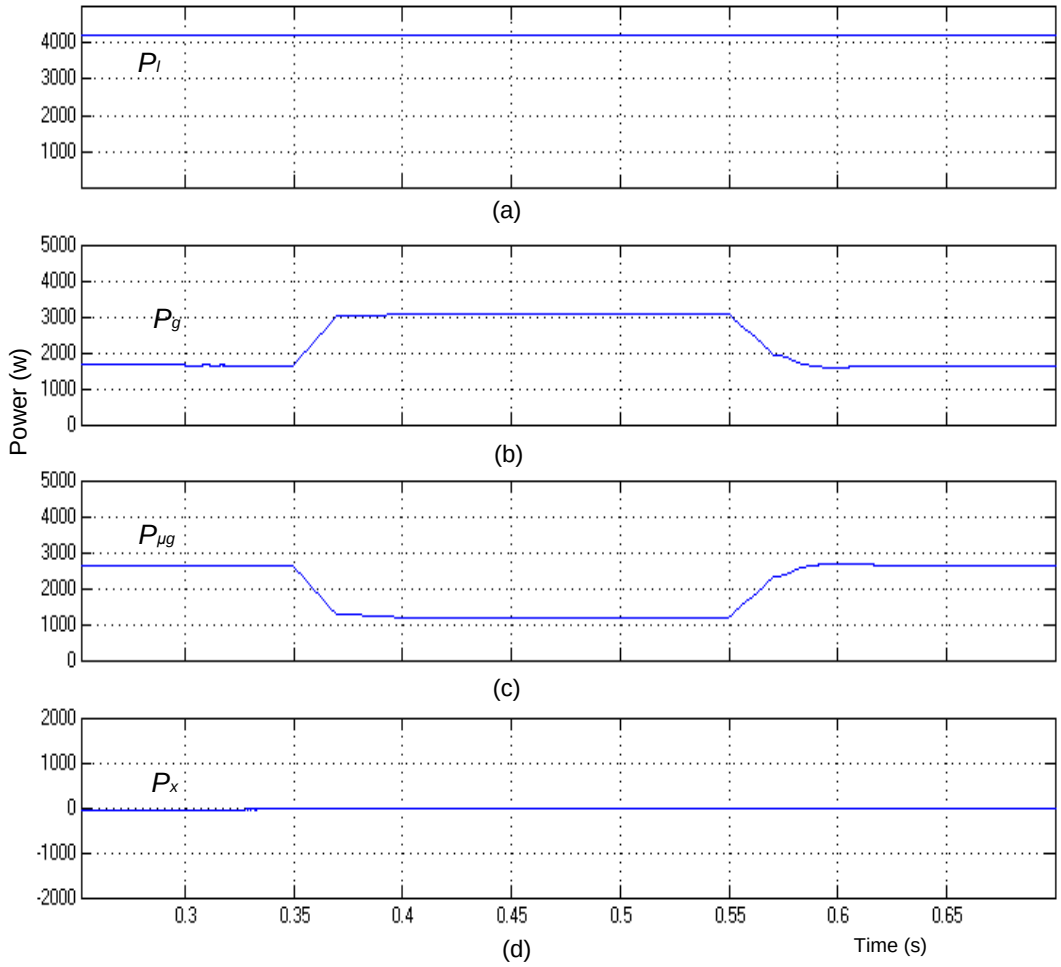

Figure 4.5: Active power sharing (a) Load active power (b) Active power supplied by grid (c) Active power supplied by MVSI (d) Active power supplied by AVSI

(v_{dcref}) of 1040V by the PI controller.

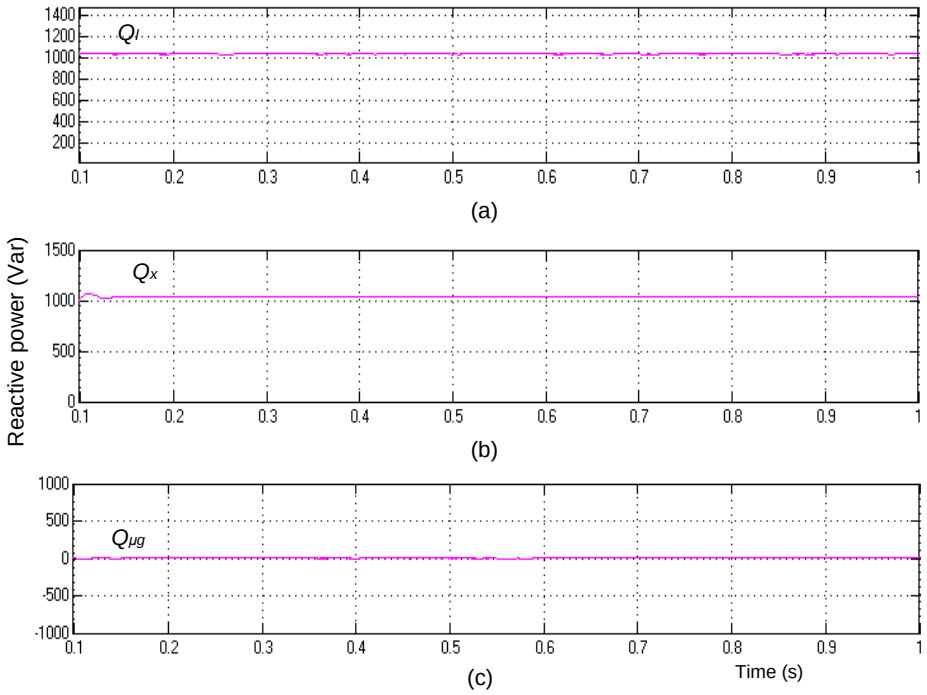

Figure 4.6: Reactive power sharing (a) Load reactive power (b) Reactive power supplied by AVSI (c) Reactive power supplied by MVSI.

4.4 Conclusions

A dual voltage source inverter scheme (DVSI) is proposed for microgrid systems with enhanced power quality. A control algorithms are developed to generate reference currents for DVSI using instantaneous symmetrical component theory (ISCT). The proposed scheme has the capability to exchange power from distributed generators (DGs) and also to compensate the local unbalanced and non-linear load. The performance of the proposed scheme has been validated through simulation studies. As compared to a single inverter with multifunctional capabilities, the DVSI has many advantages such as, increased reliability, lower cost due to the reduction in filter size and, more utilization of inverter capacity to inject real power from DGs to the microgrid. Moreover, the use of three phase, three wire topology for main inverter reduces the dc link voltage requirement. Thus, a DVSI scheme is a suitable option for microgrid supplying sensitive loads.

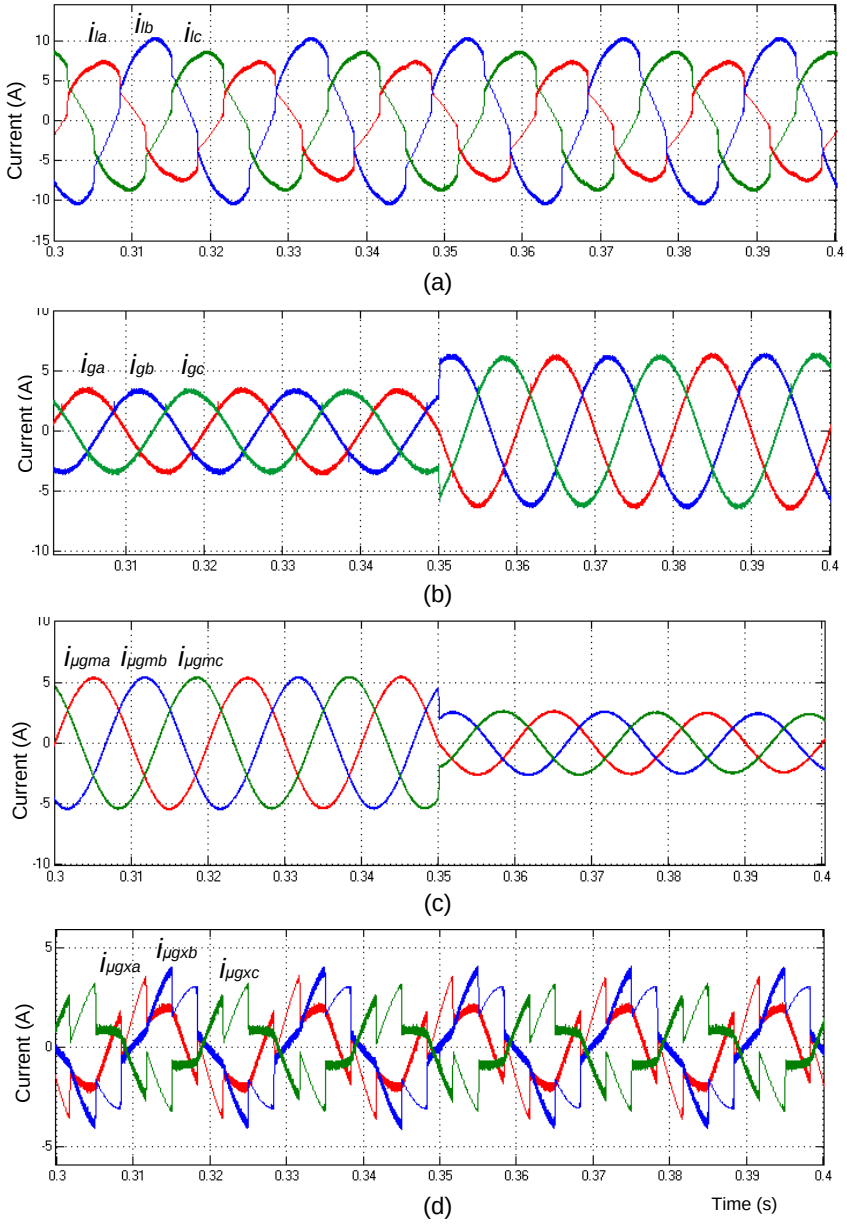

Figure 4.7: Simulated performance of DVSI scheme (a) Load currents (b) Grid currents (c) MVSI currents (d) AVSI currents.

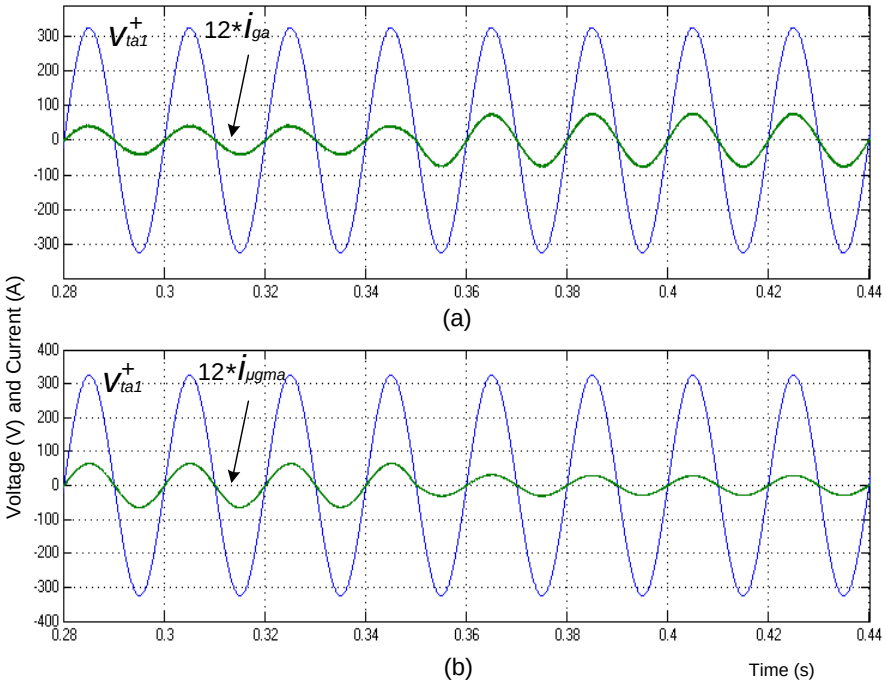

Figure 4.8: (a) PCC voltage and grid current (phase-a) (b) PCC voltage and MVSI current (phase-a).

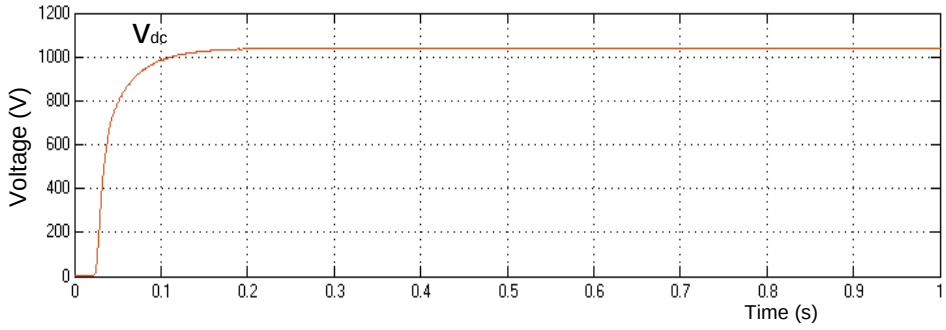

Figure 4.9: DC-link voltage of AVSI

CHAPTER 5

CONCLUSIONS AND FUTURE SCOPE

Multifunctional grid tied inverters are widely used in microgrid applications simultaneously to inject the generated power from distributed generation (DG) units and to control the power quality aspects at the PCC. The control strategies and topologies of these inverters are quite significant in deciding the power transfer and load compensation capabilities of DG interfaced distribution system. This thesis has focused on the dual voltage source inverter topology to improve the power injection and load compensation. The theoretical analysis supported with detailed simulation studies have been presented.

A dual voltage source inverter scheme (DVSI) is proposed for microgrid systems with enhanced power quality. Control algorithms are developed to generate reference currents for DVSI using instantaneous symmetrical component theory (ISCT). The proposed scheme has the capability to exchange power from distributed generators (DGs) and also to compensate the local unbalanced and nonlinear load. The performance of the proposed scheme has been validated through simulation and experimental studies. As compared to a single inverter with multifunctional capabilities, a DVSI has many advantages such as, increased reliability, lower cost due to the reduction in filter size and, more utilization of inverter capacity to inject real power from DGs to microgrid. Moreover, the use of three-phase, three-wire topology for main inverter reduces the dc link voltage requirement. Thus, the DVSI scheme is a suitable option for microgrid supplying sensitive loads.

5.1 Future Scope

Following are the future scopes of the work done in this thesis.

- The dual inverter scheme and their control algorithm discussed in this work involves the operation in grid connected mode. However, a microgrid is required to

change its operation to islanded mode, whenever a power quality event occurs at the grid level. Also, a smooth change over from grid connected mode to islanded mode has to be ensured. These aspects have to be analysed in detail.

- The dual inverter scheme uses a first order inductor filter to filter out the switching ripples generated due to the fast switching of inverter switches. The filter performance can be improved by using higher order filters like LC or LCL filter. The addition of higher order filter may affect the stability of the system.

- All control algorithms discussed in this thesis assumes a constant frequency for the source voltage. However, the frequency in a microgrid may vary within a permissible range depending on the power difference between generation and load demand. This variation in frequency has to be considered in the control algorithm for dual inverter scheme.

REFERENCES

[1] J. Nastran, R. Cajhen, M. Seliger,P. Jereb, " *Active power filter for nonlinear AC loads*", IEEE Transactions on Power Electronics, vol.9, no.1, pp. 92-96, Jan 1994.

[2] D.A. Torrey, A.M.A.M. Al-Zamel, "*A single-phase active power filter for multiple nonlinear loads*", IEEE Transactions on Power Electronics, vol.10, no.3, pp. 263-272, May 1995

[3] J. Hafner, M. Aredes, K. Heumann, "*A shunt active power filter applied to high voltage distribution lines*" IEEE Transactions on Power Delivery, vol.12, no.1, pp.266-272, Jan 1997.

[4] J. G. Nielsen, M. Newman, H. Nielsen, F. Blaabjerg, "*Control and testing of a dynamic voltage restorer (DVR) at medium voltage level*", IEEE Transactions on Power Electronics, Vol.19, no.3, pp.806-813, May 2004.

[5] H. Fujita and H. Akagi "*The unified power quality conditioner: the integration of series and shunt-active filters*", IEEE Transactions on Power Electronics, Vol. 13, No.2, pp.315-322, Mar 1998.

[6] A. A. Chowdhury, S. K. Agarwal, D. O. Koval," *Reliability modelling of distributed generation in conventional distribution systems planning and analysis*", IEEE Transactions on Industrial Applications, vol.39, no. 5, pp.1493-1498 Sept 2003.

[7] H. Akagi; Y. Kanazawa and A. Nabae, "*Instantaneous reactive power compensators comprising switching devices without energy storage components*", IEEE Transactions on Industrial Applications, vol.IA-20, no.3, pp.625-630, May 1984.

[8] A. Ghosh and A. Joshi "*A new approach to load balancing and power factor correction in power distribution system*",IEEE Transactions on Power Delivery, Vol. 15, No.1, pp.417-422, jan 2000.

[9] A. Ghosh and A. Joshi "*The use of instantaneous symmetrical components for balancing a delta connected load and power factor correction*",Electrical Power Systems Research, Vol.54, No.1, pp.67-74, 2000.

[10] M.Benhabib and S.Saadate "*New control approach for four-wire active power filter based on the use of synchronous reference frame*", Electrical Power Systems Research, vol.73, no.3, pp.353-362, 2005

[11] U.Rao, Mahesh K.Mishra and A. Ghosh "*Control strategies for load compensation using instantaneous symmetrical component theory under different supply voltages*",IEEE Transactions on Power Delivery, Vol.23, No.4, pp.2310-2317, oct 2008.

[12] H. George and Mahesh K. Mishra "*DSTATCOM topologies for three-phase high power applications*", International Journal of Power Electronics, Vol.2, No.2, pp.107-124, 2010.

[13] Sathish Kumar Kollimalla "*Doctor of philosophy thesis-Control strategies for photovoltaic and hybrid energy storage systems in DC microgrid*", Jan 2015.

[14] Manoj Kumar M.V, Mahesh K. Mishra and Chandan Kumar "*A Grid-Connected Dual Voltage Source Inverter with Power Quality Improvement Features*",IEEE Transactions on Sustainable Energy, Vol.6, No.2, pp.482-490, Apr 2015.

[15] Mahesh K. Mishra and K. Karthikeyan, "*Design and analysis of voltage source inverter for active compensators to compensate unbalanced and non-linear loads*", in Proceedings of IEEE International Power Engineering Conference, pp. 649-654, 2007.

[16] Manoj Kumar M.V, "*Doctor of philosophy thesis-Control strategies and topologies of inverters in microgrid connected power distribution system*", Sept 2015